Australian Government
Department of Defence
Defence Science and
Technology Organisation

An Experimental Investigation Into the Feasibility of Measuring Static and Dynamic Aerodynamic Derivatives in the DSTO Water Tunnel

Lincoln P. Erm

Aerospace Division
Defence Science and Technology Organisation

DSTO-TR-2600

ABSTRACT

This report gives details of an experimental research investigation carried out in the DSTO water tunnel to see whether it is feasible to measure meaningful aircraft static and dynamic aerodynamic derivatives. These derivatives represent the aerodynamic damping and coupling forces and moments on an aircraft and are used in its equations of motion. A Standard Dynamics Model (SDM), a simplified fighter aircraft configuration, was used for the tests. The SDM was subjected to forced small (±0.5°) sinusoidal pitching oscillations and derivatives were computed from measured model loads, angles of attack, reduced frequency of oscillation and aircraft geometrical parameters. The derivatives obtained in the water tunnel were compared with corresponding published data obtained using SDMs in wind tunnels. Although wind tunnels are the preferred option to obtain derivatives, it was found that it is feasible to use a water tunnel to obtain approximate derivatives, at least for models having SDM-type geometries, especially if derivatives are required quickly and cheaply.

RELEASE LIMITATION

Approved for public release

Published by

Aerospace Division
DSTO Defence Science and Technology Organisation
506 Lorimer St
Fishermans Bend, Victoria 3207 Australia

Telephone: 1300 DEFENCE
Fax: (03) 9626 7999

AR-015-088
August 2013

APPROVED FOR PUBLIC RELEASE

An Experimental Investigation Into the Feasibility of Measuring Static and Dynamic Aerodynamic Derivatives in the DSTO Water Tunnel

Executive Summary

There is a continuing requirement at the Defence Science and Technology Organisation (DSTO) to develop flight-dynamic models for modern combat aircraft to enable the behaviour of aircraft to be predicted for given control inputs. Flight-dynamic models incorporate aircraft equations of motion, which contain static and dynamic aerodynamic derivatives. These derivatives represent the aerodynamic damping and coupling loads on an aircraft performing manoeuvres.

To measure the derivatives, it is necessary to carry out tests on an aircraft when it is in motion. Ideally, tests should be done on full-size aircraft, but such testing is expensive and there is limited control over flight conditions (such as turbulence). It is more convenient and cheaper to carry out tests in tunnels. In the past, wind tunnels, rather than water tunnels, have been used due to the fact that Reynolds numbers for models in wind tunnels are closer to those for full-size aircraft than are Reynolds numbers for models in water tunnels. Reynolds numbers in wind tunnels are at least two orders of magnitude greater than those in water tunnels, resulting from using larger models and higher free-stream velocities in wind tunnels.

Nevertheless, there are some distinct advantages in using water tunnels to measure derivatives. Model rotational and translational speeds are typically 100 times slower than those used in wind tunnels and smaller and cheaper models can be used, all of which greatly simplify experimental programs. The aim of the current research investigation was to determine whether meaningful derivatives could be measured in the DSTO water tunnel.

The current experimental program to determine derivatives, including the method used to reduce data, is based on the recommendations given by Newman (2011) in his theoretical study on the measurement of derivatives. The current study complements that of Newman and his companion report should be read in conjunction with the current report.

Derivatives were measured in the water tunnel using a Standard Dynamics Model (SDM), a simplified fighter aircraft configuration. The SDM was subjected to forced small (maximum = ±0.5°) sinusoidal pitching oscillations about a fixed point and derivatives were calculated from measured model normal forces, pitching moments, angles of attack, reduced frequency of oscillation and aircraft geometrical parameters. To obtain all of the required derivatives, it was necessary to take measurements with the model mounted on stings of different lengths, which imparted differing amounts of oscillatory and plunging motion to the model. To obtain static and combined dynamic derivatives, the model was mounted on a sting and oscillated about its datum. To

obtain separated dynamic derivatives, it was also necessary to oscillate the model when it was mounted on a longer sting. It is believed that this is the first time that longitudinal separated derivatives have been measured using a SDM.

SDMs have been used in different wind tunnels around the world when measuring derivatives and there is a large body of published data available that can be used for comparison purposes to check the validity of the DSTO water-tunnel data. Measured water-tunnel derivatives were found to agree reasonably well with wind-tunnel data, suggesting that it is feasible to use a water tunnel to measure derivatives, at least for models having SDM-type geometries, especially if derivatives are required cheaply and quickly.

Author

Lincoln P. Erm
Aerospace Division

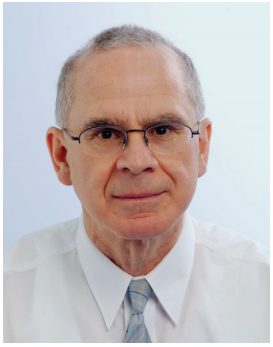

Lincoln Erm obtained a Bachelor of Engineering (Mechanical) degree in 1967 and a Master of Engineering Science degree in 1969, both from the University of Melbourne. His Master's degree was concerned with the yielding of aluminium alloy when subjected to both tensile and torsional loading. He joined the Aeronautical Research Laboratories (now called the Defence Science and Technology Organisation) in 1970 and has worked on a wide range of research projects, including the prediction of the performance of gas-turbine engines under conditions of pulsating flow, parametric studies of ramrocket performance, flow instability in aircraft intakes and problems associated with the landing of a helicopter on the flight deck of a ship. Concurrently with some of the above work, he studied at the University of Melbourne and in 1988 obtained his Doctor of Philosophy degree for work on low-Reynolds-number turbulent boundary layers. Since this time, he has undertaken research investigations in the low-speed wind tunnel and the water tunnel. Recent work has been concerned with extending the testing capabilities of the water tunnel, including developing a two-component strain-gauge-balance load-measurement system for the tunnel and developing a dynamic-testing capability for the tunnel.

This page is intentionally blank

Contents

Acronyms

AEDC	Arnold Engineering Development Centre
DFVLR	Deutsche Forschungs- und Versuchsanstalt fur Luft- und Raumfahrt (German Research & Development Institute for Air & Space Travel)
DSTO	Defence Science and Technology Organisation (Australia)
FFA	Flygtekniska Forsoksanstalten (Aeronautical Research Institute of Sweden)
NAE	National Aeronautical Establishment (Canada)
NAL	National Aerospace Laboratory (Japan)
NASA	National Aeronautics & Space Administration (USA)
SDM	Standard Dynamics Model
TPI/TU	Turin Polytechnic Institute/Technical University (Italy)

This page is intentionally blank

Nomenclature

b	Model reference wingspan, (m).
C	Coefficient used in the calibration equations for a strain-gauge balance.
C_{iq}	Dynamic derivatives due to pitch rate, $C_{iq} = \frac{\partial C_i}{\partial q}\frac{2V}{\bar{c}}$, i = X, Y, Z, l, m, n.
C_{ir}	Dynamic derivatives due to yaw rate, $C_{ir} = \frac{\partial C_i}{\partial r}\frac{2V}{b}$, i = X, Y, Z, l, m, n.
$C_{i\alpha}$	Static derivatives due to angle of attack, $C_{i\alpha} = \frac{\partial C_i}{\partial \alpha}$, i = X, Y, Z, l, m, n.
$C_{i\dot{\alpha}}$	Dynamic derivatives due to angle of attack rate, $C_{i\dot{\alpha}} = \frac{\partial C_i}{\partial \dot{\alpha}}\frac{2V}{\bar{c}}$, i = X, Y, Z, l, m, n.
$C_{i\beta}$	Static derivatives due to angle of sideslip, $C_{i\beta} = \frac{\partial C_i}{\partial \beta}$, i = X, Y, Z, l, m, n.
$C_{i\dot{\beta}}$	Dynamic derivatives due to angle of sideslip rate, $C_{i\dot{\beta}} = \frac{\partial C_i}{\partial \dot{\beta}}\frac{2V}{b}$, i = X, Y, Z, l, m, n.
C_l	Rolling-moment coefficient, (non-dimensional), $C_l = L/(0.5\rho V^2 Sb)$.
C_m	Pitching-moment coefficient, (non-dimensional), $C_m = M/(0.5\rho V^2 S\bar{c})$.
C_n	Yawing-moment coefficient, (non-dimensional), $C_n = N/(0.5\rho V^2 Sb)$.
C_X	Axial-force coefficient, (non-dimensional) $C_X = X/(0.5\rho V^2 S)$.
C_Y	Side-force coefficient, (non-dimensional), $C_Y = Y/(0.5\rho V^2 S)$.
C_Z	Normal-force coefficient, (non-dimensional), $C_Z = Z/(0.5\rho V^2 S)$.
C_{Z0}	Normal-force coefficient in steady reference condition, (non-dimensional).
$\bar{c}$	Mean aerodynamic chord (MAC) of a model, (m).
d	Model fuselage base diameter, (m).
f	Equivalent constant circular frequency of rotation for oscillatory pitching motion, (Hz).
H	Load applied to a strain-gauge balance, (N).
k	Reduced frequency of oscillation of a model, (non-dimensional), $k = \omega\bar{c}/2V$ for pitching motion, $k = \omega b/2V$ for rolling and yawing motion.
L	Rolling moment associated with the model and the balance coordinate systems, (N·m), (see Figures 1 and 4).
l_b	Displacement of the SDM datum forward of the balance calibration reference centre, (m).
l_c	Displacement of the SDM datum forward of the centre of rotation of the dynamic-rig motion system, i.e. from the centre of the imaginary circle formed by the C-strut, (m), (see Figure 9).

M	Pitching moments associated with the model and the balance coordinate systems, (N·m), (see Figures 1 and 4).
M_t	Mach number, (non-dimensional).
N	Yawing moment associated with the model and the balance coordinate systems, (N·m), (see Figures 1 and 4).
p	Rolling angular velocities about the x axis, (radians/s), (see Figure 1).
q	Pitching angular velocity about the y axis, (radians/s), (see Figure 1).
R	Electrical resistance of a strain-gauge, (Ω).
R	Voltage ratio, $R = V_{OUT}/V_{IN}$.
Re	Reynolds number, (non-dimensional), $Re = \rho \bar{c}\ V/\mu$.
r	Yawing angular velocity about the z axis, (radians/s), (see Figure 1).
S	Reference area of a model, (m^2).
V	Speed of a body with respect to a fluid, (m/s).
X	Axial force associated with the model and the balance coordinate systems, (N), (see Figures 1 and 4).
x, y, z	Axes for the model and balance coordinate systems, right-handed (see Figures 1 and 4).
x_a, y_a, z_a	Axes for the air-path coordinate systems, right-handed, (see Figure 2).
Y	Side force associated with the model and the balance coordinate systems, (N), (see Figures 1 and 4).
Z	Normal force associated with the model and the balance coordinate systems, (N), (see Figures 1 and 4).

Greek Letters

α	Angle of attack, (degrees).
$\dot{\alpha}$	Rate of change of angle of attack, (radians/s).
β	Angle of sideslip, (degrees).
$\dot{\beta}$	Rate of change of angle of sideslip, (radians/s).
Δ	Perturbation quantity prefix.
θ	Pitch angle, (degrees).
θ_A	Pitch angle oscillation amplitude, (degrees).
θ_0	Mean pitch angle, (degrees).
μ	Dynamic viscosity of air or water, (kg/(m·s)).
ρ	Density of air or water, (kg/m^3).
ϕ	Roll angle, (degrees).
ψ	Yaw angle, (degrees).
ω	Angular rate associated with frequency of oscillation, $\omega = 2\pi f$, (radians/s).

1. Introduction

There is an ongoing need at the Defence Science and Technology Organisation (DSTO) to develop simplified flight-dynamic models for modern highly-manoeuvrable combat aircraft to predict their behaviour for given control inputs. Such models incorporate databases of aircraft aerodynamic characteristics, including static and dynamic aerodynamic derivatives, used in the equations of motion for the aircraft. These derivatives represent the aerodynamic damping and coupling forces and moments on aircraft. An aerodynamic derivative is a concept whereby an aerodynamic force or moment is expressed as a function of one or more state vector components. For example, an incremental change in the pitching-moment coefficient can be regarded as a function of the angle of attack, i.e. $\Delta C_m = C_{m_\alpha} \Delta\alpha$, where the aerodynamic derivative C_{m_α} is given by $\partial C_m / \partial \alpha$. Aerodynamic derivatives are locally linearised quantities which are only valid in the linearised region.

Whenever a flight-dynamic model is developed for a new aircraft, there is a need to acquire derivative data to populate the database. This could be done by carrying out tests on full-size aircraft in flight, but this is expensive and time consuming. It is far cheaper and more convenient to obtain the data from tests in tunnels. The proviso of course is that lack of Reynolds-number similarity between tunnel tests and operation of full-size aircraft does not adversely affect the validity of the tunnel data. One of the most widely used methods to obtain derivatives in tunnels is the direct forced-oscillation technique, whereby a model is oscillated at a constant small amplitude (typically about $\pm 1.0°$) and a constant frequency in a single degree of freedom, such as pitch or plunge. The aerodynamic reaction is therefore directly connected to the motion. For such motion, by measuring instantaneous model normal forces, pitching moments and angles of attack, as well as reduced frequency of oscillation and aircraft geometrical parameters, it is possible in principle to obtain longitudinal aerodynamic derivatives, without the need to solve the aircraft equations of motion.

In the past, derivatives have generally been measured using wind tunnels, rather than water tunnels, due to the fact that Reynolds numbers for models in wind tunnels are closer to those for full-size aircraft than are Reynolds numbers for models in water tunnels. Reynolds numbers in wind tunnels are at least two orders of magnitude greater than those in water tunnels, resulting from using larger models and higher free-stream velocities in wind tunnels. Flow-induced loads on models in water tunnels are very small and in the past have been difficult to measure accurately. However, using modern semi-conductor strain gauges, such loads can now be measured accurately. Water tunnel models can also be manufactured far quicker and cheaper than wind tunnel models. Model rotation rates required in water tunnels to achieve dynamic similarity are typically two orders of magnitude less than those required for tests in wind tunnels, which simplifies testing. Using water tunnels to acquire static and dynamic aerodynamic derivatives may now be a viable option.

This report gives details of an experimental investigation undertaken in the DSTO water tunnel to assess whether it is feasible to measure longitudinal static and dynamic aerodynamic derivatives in the tunnel using a Standard Dynamics Model (SDM). The experimental program, including data processing, is based on the recommendations given by Newman (2011) in his theoretical study on the measurement of derivatives. Readers are advised to read Newman's report in conjunction with the current report to familiarise themselves with his methodology.

The SDM was subjected to forced small simple-harmonic oscillations in combined pitch and plunge using a dynamic-testing system specially built for the water tunnel (see Erm, 2006a, 2006b). Data were acquired while the model was in motion, enabling longitudinal static and dynamic derivatives, including separated dynamic derivatives, to be calculated. Derivatives measured using the SDM in the water tunnel were compared with corresponding published data obtained using SDMs in wind tunnels to check the accuracy of the water-tunnel data.

2. Standard Dynamics Model

In 1978, staff at the National Aeronautical Establishment (NAE), Canada, conceived and developed a simplified fighter aircraft configuration for their testing programs. Subsequently, recognizing the need for establishing the validity of new dynamic-stability test techniques, the NAE concept was adopted by NASA Ames and the Arnold Engineering Development Center (AEDC) as a basis for a standard model to be tested in different wind-tunnel facilities. Beyers & Moulton (1983) outline the history of the model. It is now known as the Standard Dynamics Model, or SDM, and has the shape shown in Figure 1. It has an axisymmetric fuselage and flat tapered lifting surfaces, with span- and chord-wise tapered leading and trailing edges. The body has an ogive-cylinder profile and incorporates a tapered intake unit with a forward-facing flat face and a biconvex circular canopy. Since its inception, the SDM has been widely used around the world by different researchers in different wind-tunnel facilities when acquiring experimental static and dynamic aerodynamic derivatives. Consequently, there is a significant body of SDM wind-tunnel derivative data available in the literature, which can be used for comparison purposes to assess the goodness of the DSTO SDM water-tunnel data. This is the main reason why the SDM has been used in the current study rather than later advanced aircraft models.

The SDM used in the DSTO water tunnel was manufactured using stereolithographic techniques. The model as supplied contained small steps in its surfaces, due to the manufacturing technique used, which were lightly filled and smoothed by hand. The model was painted matt black to waterproof it and to provide a suitable contrasting background for possible future flow-visualisation studies. No dye ports or pressure ports were embedded in the model during manufacture, but a cavity was designed into the

model along its centreline, enabling a metal sleeve to be fitted to accommodate a strain-gauge balance.

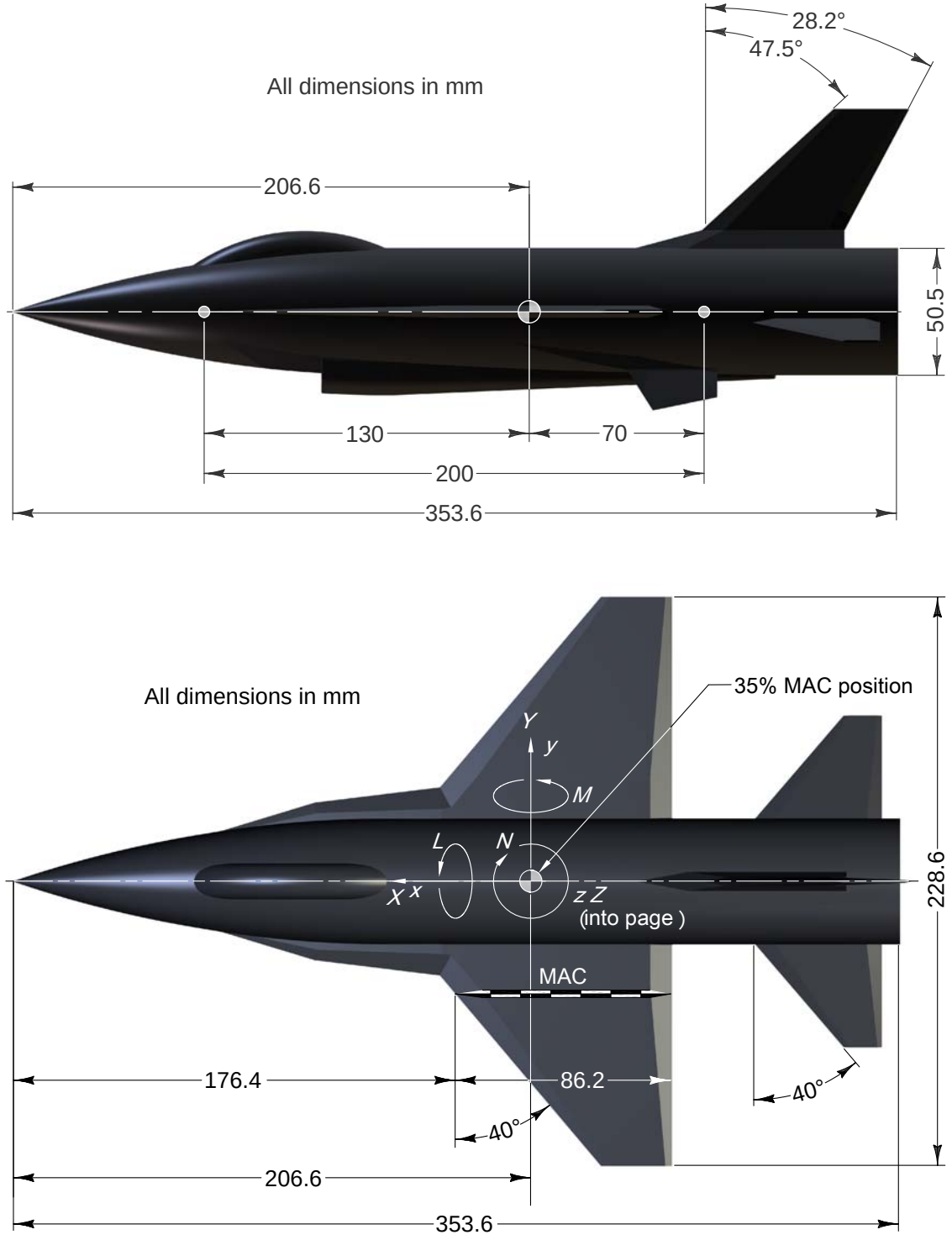

Figure 1. Standard Dynamics Model, showing the location of the model datum, the coordinate system and the fluorescent markers (solid circles on side view of model).

As shown in Figure 1, the SDM used in the water tunnel has a wing span, b, of 228.6 mm and a mean aerodynamic chord (MAC), $\bar{c}$, of 86.2 mm. The water-tunnel model is the same size at that used by Beyers & Moulton, 1983, Beyers *et al*., 1984 and Huang & Beyers, 1990 in wind tunnels. The geometric fidelity of the water-tunnel SDM (preciseness of overall shape, including matched sharpness of leading edges) is of some concern. The water-tunnel SDM was made from resin using stereolithographic techniques, rather than being machined from metal. The SDMs used in the wind-tunnel investigations were up to about 3 times as large as the water-tunnel SDM (see Table 1). Consequently, the water-tunnel model may not have been manufactured to the same precision as the wind-tunnel models.

Two fluorescent markers, located 200 mm apart (nominal distance), were positioned on the model as shown. These markers were used to determine the offset of the SDM datum relative to the centre of rotation of the dynamic-rig motion system when the SDM is mounted on the rig for testing (see Section 6.2 for details of the offset).

Details of the location of the SDM datum and the right-handed orthogonal body-coordinate system (x, y, z) are shown in Figure 1, along with the corresponding notation used for forces and moments. The relationship between the wind (air-path) coordinate system and the body coordinate system is shown in Figure 2. The angles of attack, α, and sideslip, β, are defined in terms of the two coordinate systems as shown.

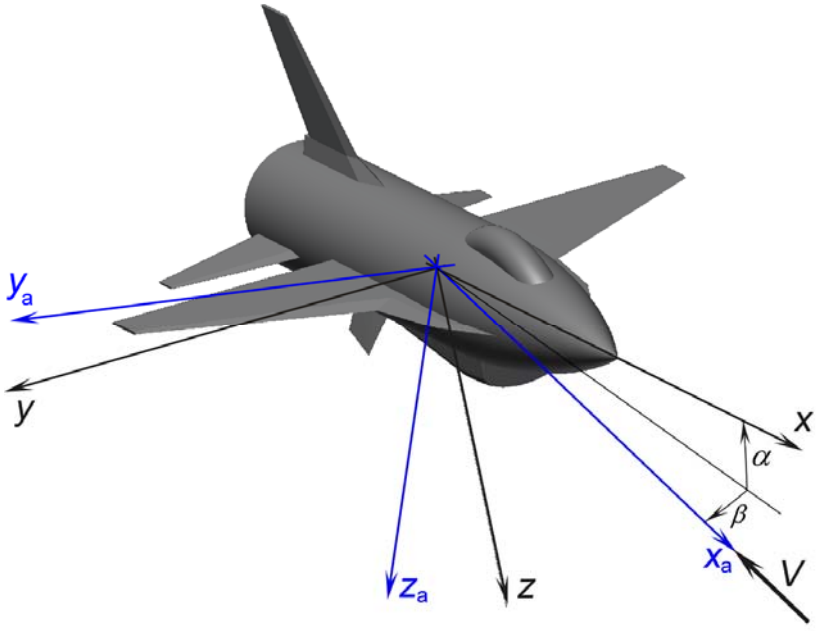

Figure 2. Standard Dynamics Model, showing the relationship between the wind (air-path) coordinate system and the body coordinate system.

3. DSTO Water Tunnel and Ancillary Equipment

3.1 Water Tunnel

The DSTO water tunnel was manufactured by Eidetics International Incorporated [1] and is designated Model 1520. The tunnel, shown in Figure 3, holds about 3790 litres of water and has a horizontal-flow test section 380 mm wide, 510 mm deep and 1630 mm long. It is a recirculating closed-circuit tunnel and there is a free water surface in the test section. The free-stream velocity in the test section can be varied up to 0.6 m/s. The side walls and floor of the test section are made from glass to facilitate flow-visualization studies. The tunnel is constructed so that it is possible to look directly upstream into the test section through a glass window at the downstream end of the diffuser. Downstream of the settling chamber there are flow-conditioning elements, consisting of a perforated stainless-steel plate, a honeycomb and two fibreglass screens. The one-dimensional contraction upstream of the test section has an inlet/outlet area ratio of 6:1. This geometry gives a good velocity distribution and turbulence level, and avoids the likelihood of local flow separations. According to the Eidetics Water Tunnel Operations Manual, the free-stream velocity in the test section varies by less than ±2% relative to the average value, the mean flow angularity is within the range ±1.0° in both pitch and yaw angles, and the turbulence intensity is less than 1.0% RMS.

Models are mounted on a C-strut so that the required centre of rotation of a model is at the centre of the imaginary circle formed by the strut, ensuring that all angular motion of the model is about this point. With the current model supporting system, it is only possible to rotate a model in roll, pitch and yaw. Plunging of the model is not possible. The supporting system is attached to the top of the test section by a hinge, so that a model can be lowered into the test section, or removed from the test section, as required. When a model has been lowered, its centre of rotation is at the mid transverse position in the test section, 270 mm from the floor and 965 mm downstream of the start of the test section.

A Dynasonics™ Series TFXD Transit Time Ultrasonic Flow Meter was used to measure test-section free-stream velocities. The system utilises two transducers that are glued onto the wall of the test section, at a known distance apart, and function as both ultrasonic transmitters and receivers. The system operates by alternatively transmitting and receiving a frequency modulated burst of sound energy between the two transducers and measuring the time interval that it takes for sound to travel between the transducers. The difference in the measured time interval is directly related to the average free-stream velocity across the test section.

1 Now called Rolling Hills Research Corporation, 420 N. Nash St., El Segundo, CA 90245, USA.

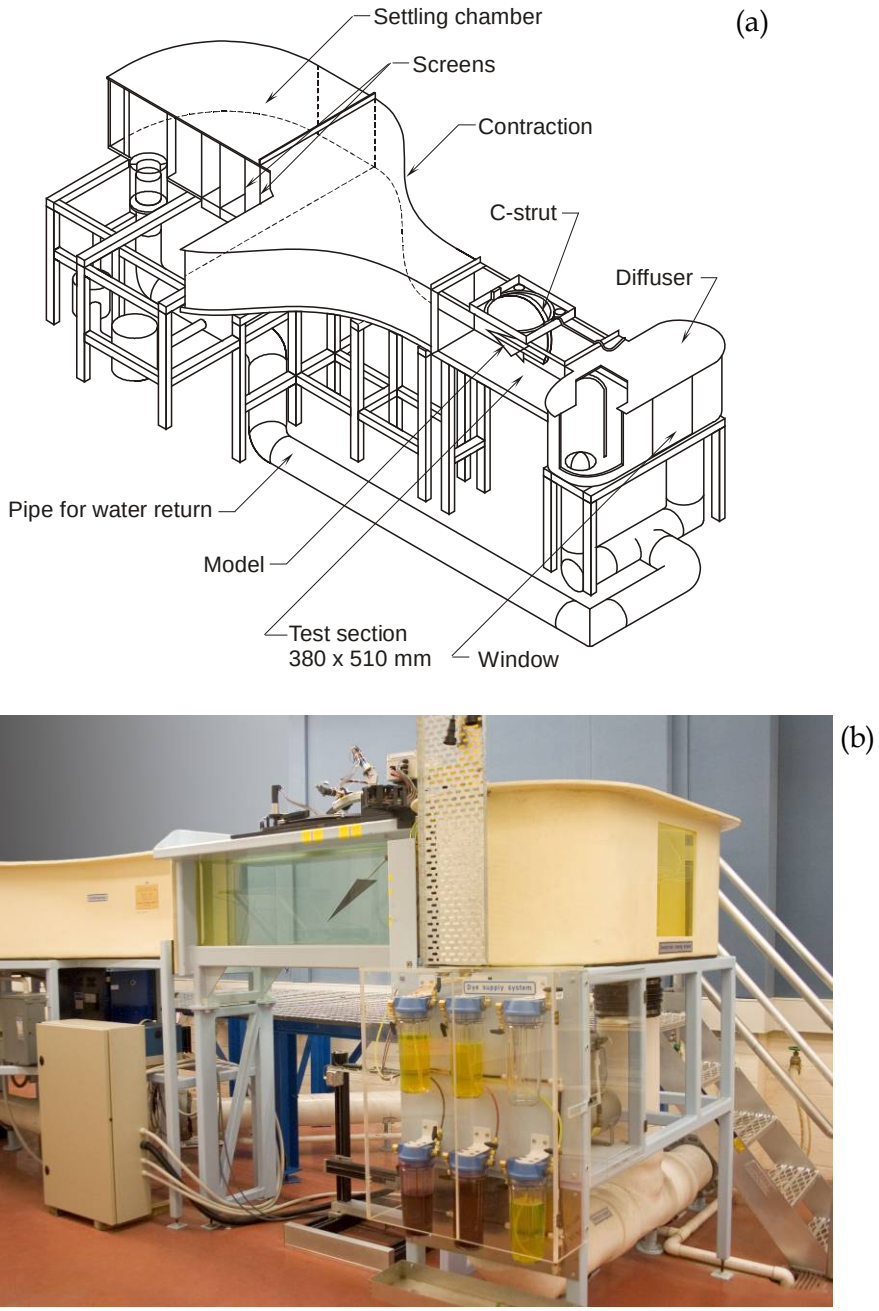

Figure 3. Eidetics Model 1520 water tunnel; (a) diagrammatic view of tunnel, (b) photograph of tunnel.

3.2 Load-Measurement System

A load-measurement system has been developed to measure the very small forces and moments on a model in the water tunnel. The system is comprised of a sensitive low-range two-component strain-gauge balance, a bridge-conditioner unit, a rig to calibrate the balances and a PC-controlled data-acquisition system.

3.2.1 Two-Component Strain-Gauge Balance

A diagrammatic representation of the two-component balance, showing the position of the gauges and the coordinate system, is given in Figure 4. For completeness, the full conventional set of axes and loads are given, but the balance can only measure normal forces (Z) and pitching moments (M). The two-component balance has been designed to measure normal forces and pitching moments within the ranges ±2.5 N and ±0.02 N·m respectively. Due to the small loads, semi-conductor strain gauges have been used, having a resistance of 1000 Ω, a gauge factor of 145, and active dimensions of 1.27 mm by 0.15 mm. The gauges were manufactured by PSI-TRONIX Incorporated[2] and their specification is P01-05-1000. The balance contains four gauges on each of the two sides of the flexure member, as shown. Gauges 1b, 1c, 2d and 2b, which are obscured, are on the opposite side of the flexure member directly underneath gauges 1a, 1d, 2a and 2c respectively. The four gauges in each set are connected together to form two Wheatstone bridges, as shown. The gauges and the connecting leads have been waterproofed by coating them with a compound designated M-coat C[3], a solvent-thinned (naptha) room-temperature-vulcanizing silicone rubber.

3.2.2 Bridge-Conditioner Unit

A Bridge-Conditioner Unit (BCU) (not shown) was used to supply input voltages to the Wheatstone bridges on the balance, as well as to null (i.e. set the bridge output voltages close to 0.0 V), amplify and filter output voltages from the bridges, before the signals were sampled by a PC-based data-acquisition system (see Section 3.2.4). The BCU was controlled using the graphical-user interface (GUI) shown in Figure 5. The unit incorporates 12 channels, but only 4 channels are shown on the interface at any given time. By clicking radio buttons on the GUI, the BCU can null the output voltages from the Wheatstone bridges and digitally set the amplifier gains. The output voltages can also be nulled by pressing a button on the BCU. The gains that can be selected on the interface vary from 1 to 100, but it is important to note that the selected gains have to be multiplied by 12.4 (governed by the gains of the amplifiers in the BCU) to give the actual gains, which can vary from 12.4 to 1240. The BCU contains analog filters, which incorporate a fifth-order polynomial that is representative of a Butterworth filter. Roll-off frequencies can be changed by the BCU by manually entering the values required, between 1 Hz and 100 Hz, on the GUI. The filters can be bypassed by setting the cut-off frequency to 2 kHz.

[2] PSI-TRONIX Incorporated, 3950 South "K" Street, Tulare, CA, 93274, USA.
[3] M-Coat C is manufactured by Vishay.

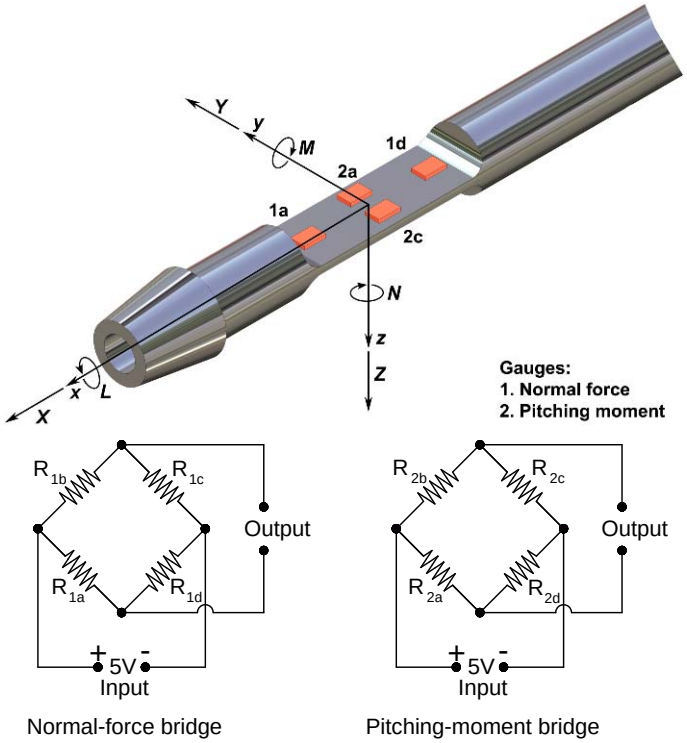

Figure 4. Two-component balance, showing the position of the gauges for the normal-force and pitching-moment channels, together with the corresponding Wheatstone- bridge circuits.

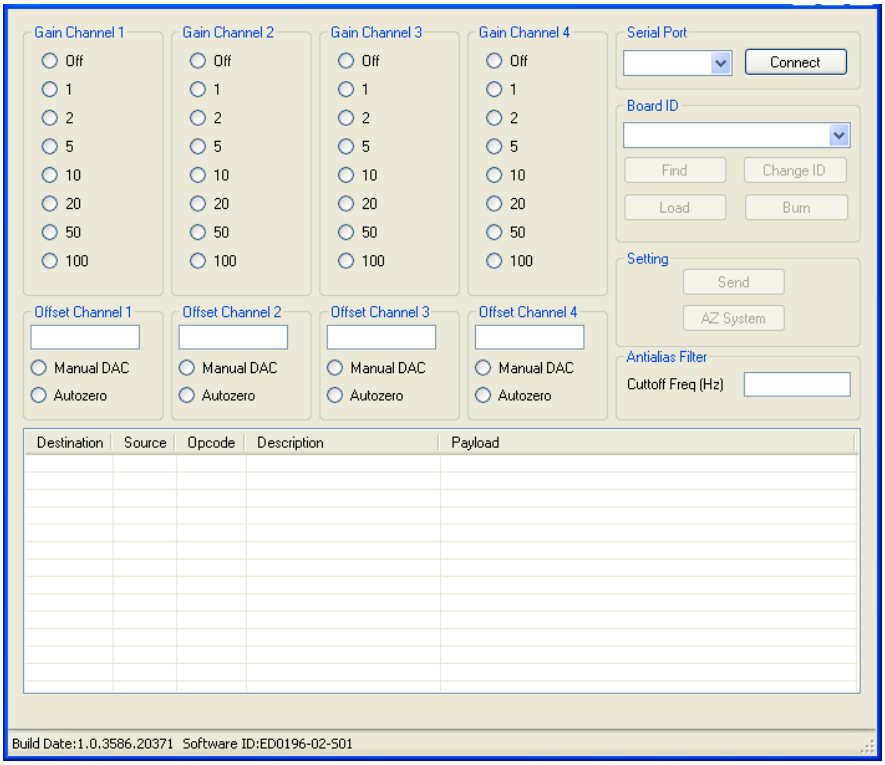

Figure 5. Graphical-user interface used to control the Bridge-Conditioner Unit.

3.2.3 Balance Calibration Rig

The two-component balance was calibrated manually using a conventional dead-weight procedure, as shown in Figure 6. A cage was attached to the balance and a pan was suspended from a knife edge along the top of the cage. Weights were progressively added to the pan, and then progressively removed, to apply forces and moments to the balance, for the pan located at different x positions along the knife edge. Bridge output voltages associated with each weight were measured, enabling the calibration coefficients to be determined. The mathematical model chosen for the calibration equations is of the form $R_i = \sum C_{i,j} H_j$, i = 1, 2 and j = 1, 2, i.e. first-order equations, where R_i are the voltage ratios (bridge output voltages divided by bridge supply voltages), $C_{i,j}$ are the calibration coefficients and H_j are the applied load components. The normal forces can be measured to an accuracy of ±0.8% and the pitching moments to an accuracy of ±0.3% of their true values.

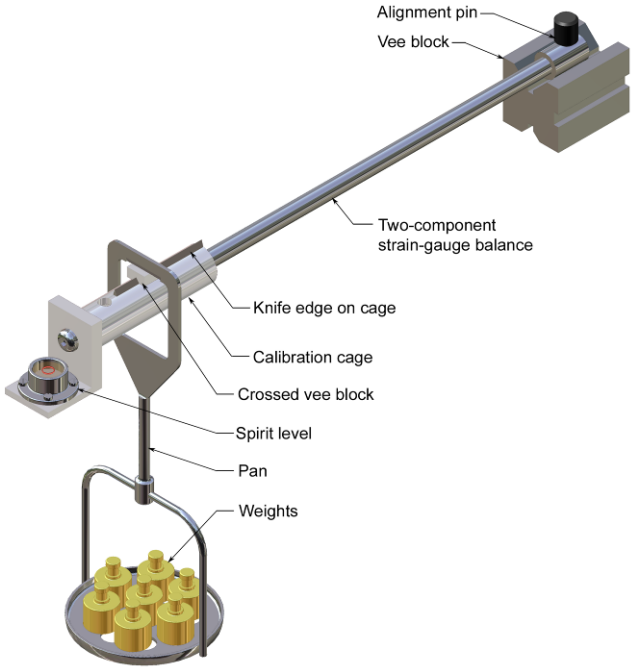

Figure 6. Experimental setup used when calibrating the two-component balance.

3.2.4 PC and Data-Acquisition Card

The PC used has a Windows™ XP Professional operating system, a Core 2 Duo 2.4 GHz CPU, a 750 GB hard disk drive, plus a 250 GB backup, and 2 GB of RAM.

The data-acquisition card interfaced with the PC was manufactured by National Instruments™ and the product code is NI 6013. The card features 16 channels (8 differential) of 16-bit analogue input, a 68 pin connector and 8 lines of digital input/output. Analogue input voltages varying between –5 V and +5 V can be sampled. For the 16-bit card, the resolution of the sampled voltages is $10.0/2^{16}$, i.e. 10.0/65536 = 0.000153 V/LSB = 0.153 mV/LSB (LSB denotes least significant bit).

3.3 Dynamic-Testing System

A PC-based dynamic-testing system has been developed for the water tunnel that enables flow-induced forces and moments on a model to be measured while it is in motion undergoing a predetermined dynamic manoeuvre in roll, pitch and yaw.

The setup of the dynamic-rig motion system is shown in Figure 7. The SDM is mounted on a strain-gauge balance which in turn is attached to a C-strut. For the case shown, the SDM is mounted so that 3 reference centres, *viz*. (1) the centre of rotation of the dynamic-rig motion system, (2) the SDM datum and (3) the balance calibration reference centre, are nominally coincident. Roll, pitch and yaw angles can be varied between 0° and ±360°, -20° and 55°, and -20° and +20° respectively. The required model roll, pitch and yaw angles at chosen instants of time throughout a dynamic manoeuvre are specified by the operator. The range of rotary motions available is virtually unlimited, and includes sinusoidal pitching oscillations used in the current testing program. The maximum obtainable roll, pitch and yaw rotational speeds of a model are ±12 degrees/s, ±6 degrees/s and ±8 degrees/s respectively. It is not possible to impart a linear plunging motion to a model, although circular plunging motion can be obtained by mounting a model on an extended (or shortened) sting, so that the model no longer rotates about the centre of rotation of the dynamic-rig motion system.

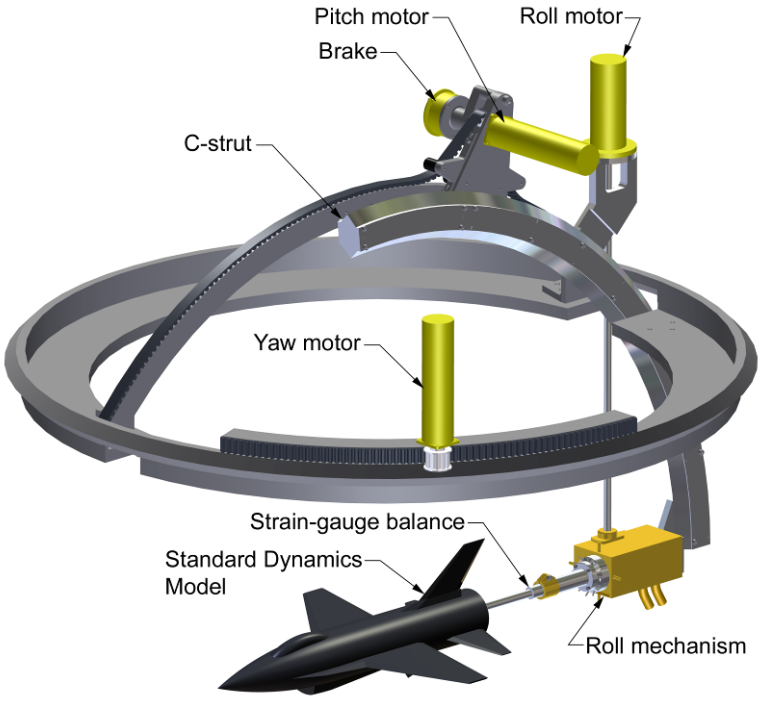

Figure 7. Diagrammatic representation of the dynamic-rig motion system.

The operation of the dynamic rig was controlled via a PC using the GUI shown in Figure 8. The interface was used to set the tunnel free-stream velocity, to set and control the model motion, and to set the sampling rates and number of samples required when sampling

voltages from a strain-gauge balance. Throughout a dynamic test, the GUI displayed instantaneous information including tunnel free-stream velocity, roll, pitch and yaw angles of the model, and balance output voltages.

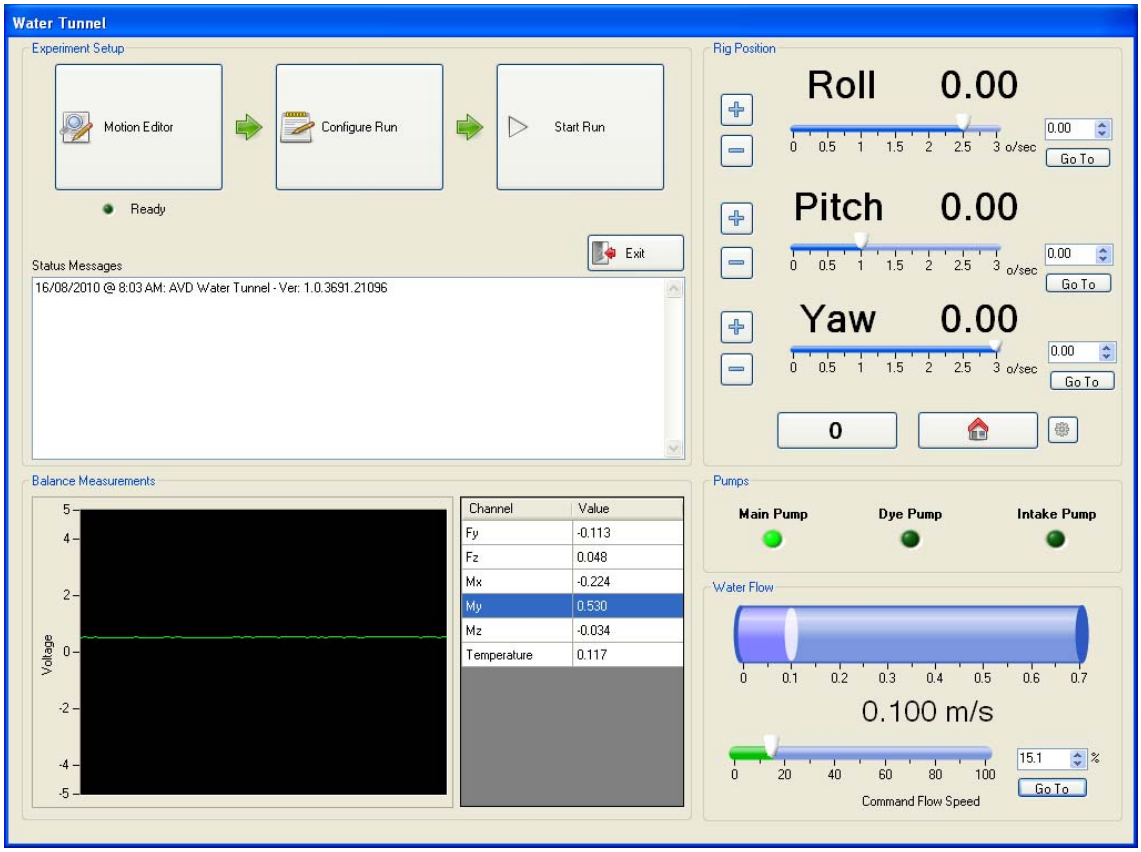

Figure 8. Graphical-user interface used when carrying out tests.

4. Basis and Implementation of Dynamic Test Technique

The experimental program to determine static and dynamic aerodynamic derivatives in the water tunnel, including data processing, is based on the methodology developed by Newman (2011). Full details of his work are not reproduced in the current report. Readers are advised to read Newman's report in conjunction with the current report to familiarise themselves with his methodology.

An underlying assumption of Newman's approach is that the equations of motion of an aircraft can be written in a linearised form in which aerodynamic coefficients are represented in terms of the aircraft state and its derivatives. For example, the linearised equation for the normal-force coefficient, C_Z, may be written as (see Newman, 2011)

$$C_Z = C_{Z0} + C_{Z\alpha}\alpha + C_{Zq}\frac{q\bar{c}}{2V} + C_{Z\dot{\alpha}}\frac{\dot{\alpha}\bar{c}}{2V} \quad (1)$$

where C_{Z0} is the normal-force coefficient in a steady reference condition. $C_{Z\alpha}$ is a static derivative, and C_{Zq} and $C_{Z\dot{\alpha}}$ are dynamic derivatives. The derivatives are given respectively by

$$C_{Z\alpha} = \frac{\partial C_Z}{\partial \alpha} \quad (2)$$

$$C_{Zq} = \frac{\partial C_Z}{\partial q}\frac{2V}{\bar{c}} \quad (3)$$

$$C_{Z\dot{\alpha}} = \frac{\partial C_Z}{\partial \dot{\alpha}}\frac{2V}{\bar{c}} \quad (4)$$

The rate derivatives have been non-dimensionalised using $2V/\bar{c}$. Similar equations can be written for the other coefficients. Such equations are used extensively in flight-dynamics modelling. They are only applicable for small disturbances about an operating point and are based on the assumption that the flight characteristics of an aircraft remain linear with change.

The two important modes of motion needed to determine longitudinal derivatives are plunge and pitch. Although the dynamic-rig motion system is not capable of plunging motion, a model mounted on a sting of length such that the model datum is not located at the centre of rotation of the dynamic-rig motion system (i.e. not located at the centre of the imaginary circle formed by the C-strut) can experience both harmonic pitching and plunging motion. The resulting combined loads may be apportioned between the two modes of motion to isolate individual derivative effects.

When measuring longitudinal derivatives, the SDM was attached to the dynamic-rig motion system using stings of different lengths (which includes using no sting extension) and oscillated with simple harmonic motion in pitch. Figures 9a and 9b show the model mounted using no sting extension and a 300 mm sting extension respectively. The amplitude of the pitching oscillations used in the tests was ±0.5°, but the amplitudes depicted in Figures 9a and 9b has been exaggerated for clarity. The Newman (2011) method of analysis relies on the linear aerodynamic assumption that the flow over a model undergoing small oscillations when mounted on an extended sting is a linear combination of the flow over the model when it is pitching about its datum and the flow over the model when it is undergoing heaving motion. This assumption is true for attached flow, but is only approximate for separated flow.

During tests, it was necessary to measure time-correlated sequences of normal forces, pitching moments, pitch angles and free-stream velocities, as well as water temperature

and atmospheric pressure. The measured data were processed using a Matlab® program developed by Newman (2011). To extract static coefficients, C_Z and C_m (measured dynamically), as well as static and combined dynamic derivatives, C_{Z_α}, C_{m_α}, $C_{Z_q}+C_{Z_{\dot\alpha}}$, $C_{m_q}+C_{m_{\dot\alpha}}$, it was only necessary to carry out tests using no sting extension. To measure separated dynamic derivatives, C_{Z_q}, $C_{Z_{\dot\alpha}}$, C_{m_q} and $C_{m_{\dot\alpha}}$, it was necessary to carry out tests using two different sting lengths, which includes the case of no sting extension. When running the program, it was possible to enter small setup corrections to allow for the fact that the SDM datum and the balance calibration reference centre were not coincident with the centre of rotation of the dynamic-rig motion system –see Section 6.2.

There are three main areas of concern when measuring aerodynamic derivatives in the water tunnel:

(1) the flow physics for the SDM in the water tunnel may not be representative of the flow physics for SDMs in the wind tunnels, due to a mismatch in Reynolds numbers (water-tunnel Reynolds number is typically 2 to 3 orders of magnitude smaller than wind-tunnel Reynolds numbers),

(2) if the flow over the SDM becomes excessively non-linear, then the linearised mathematical model used in Newman's approach (relationships such as equation 1) will break down,

(3) the data-processing techniques used by Newman may not be able to give meaningful derivatives (especially separated derivatives) if the raw data associated with a sinusoidally-oscillating model contains excessive perturbations, due to unsteady turbulent flow over the model (especially at the higher values of α), as well as inevitable noise associated with the tests. Due to the very small flow-induced loads on the water-tunnel model, noise on the raw data has a greater adverse affect on the accuracy of measured derivatives compared with associated wind-tunnel data.

It is not possible to measure lateral-directional derivatives with the two-component balance. To measure these derivatives, it would be necessary to use a five-component balance.

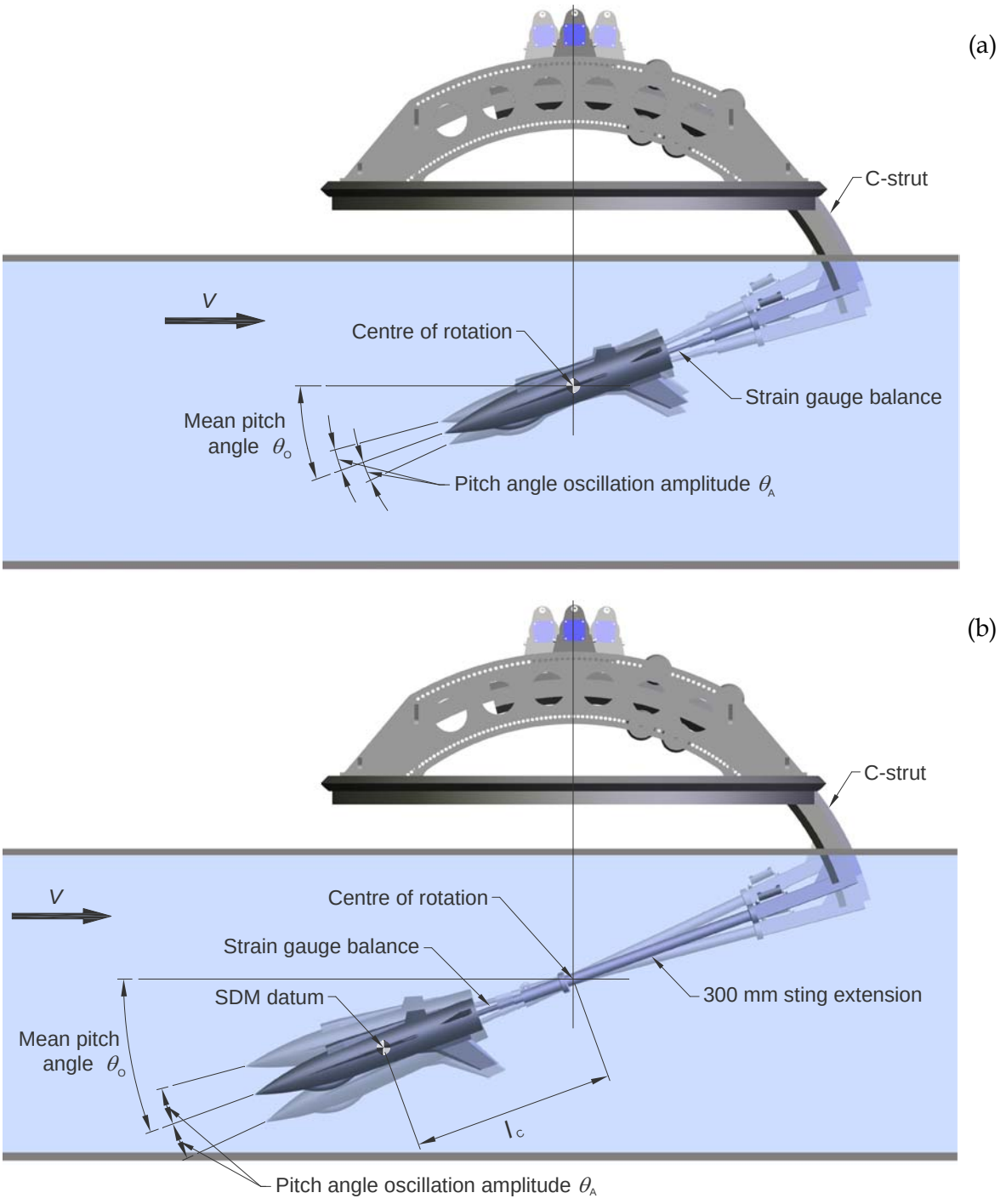

Figure 9. Geometry and kinematics of the SDM mounted on the dynamic-rig motion system. (a) no sting extension, (b) 300 mm sting extension.

5. Previous Experimental Work on Measuring Aerodynamic Derivatives Using a SDM

Previous published experimental work on measuring static and dynamic aerodynamic derivatives using the SDM is reviewed below. Most of the review will be concerned with the measurement of longitudinal derivatives, associated with longitudinal motion, i.e. linear motion along the x and z axes, and rotational motion about the y axis. However, the review will also cover some work on the measurement of lateral-directional derivatives, associated with lateral-directional motion, i.e. linear motion along the y axis, and rotational motion about the x and z axes. Research investigations are dealt with in chronological order for both high-speed and low-speed flows. The main features of the experimental investigations described below are summarised in Tables 1a and 1b for high-speed and low-speed flows respectively.

5.1 High-Speed Flows

Cyran (1981) conducted tests using a SDM in the 4 foot transonic Aerodynamic Wind Tunnel at the AEDC. The model had a wing span, b, of 19.8 inches (502.9 mm), a base diameter, d, of 4.375 inches (111.1 mm) and a MAC, $\bar{c}$, of 7.468 inches (189.7 mm), and was subjected to forced oscillations in pitch and yaw. Tests were done at Reynolds numbers per foot varying from 0.5×10^6 to 5.0×10^6, and Mach numbers varying from 0.3 to 1.3. Data were taken for angles of attack ranging from –6° to +25°. For the pitching oscillations, reduced frequencies of oscillation, $\omega d/2V$, varied from 0.009 to 0.032 ($\omega \bar{c}/2V$ varied from 0.015 to 0.055 respectively), and the oscillation amplitudes were ±1.0°, ±1.5° and ±2.0° A wide range of pitch and yaw parameters were measured, including normal-force and pitching-moment coefficients, C_Z and C_m respectively, as well as stiffness derivatives, C_{m_α}, and damping derivatives, $C_{m_q} + C_{m_{\dot{\alpha}}}$.

Coulter & Marquart (1982) conducted tests in the same tunnel and using the same SDM as Cyran (1981). The model was subjected to forced oscillations in roll, pitch and yaw. Tests were done at Reynolds numbers varying from 0.62×10^6 to 1.56×10^6, and Mach numbers varying from 0.3 to 1.3. Data were taken for angles of attack ranging from –4° to +24°, at a nominal oscillation amplitude of ±1.0°, with some data taken at amplitudes of ±0.5° and ±1.5°. The pitch, roll and yaw data were obtained at nominal oscillation frequencies of 7.5 Hz, 8.5 Hz and 3.5 Hz respectively. The researchers measured a wide range of roll, pitch and yaw parameters, including pitching-moment coefficients, C_m, and as well as static and dynamic derivatives, including stiffness derivatives C_{m_α} (measured dynamically) and damping derivatives $C_{m_q} + C_{m_{\dot{\alpha}}}$.

Beyers & Moulton (1983) carried out experiments with a SDM, having a wing span, b, of 228.6 mm, in the 0.75 m by 0.40 m Dynamics Wind Tunnel at the NAE, Canada. The model was attached to a five-component balance and mounted on a special rig that enabled it to be subjected to forced roll oscillations about the roll axis for a range of pitch and yaw angles. The test Reynolds number per metre was 10.3×10^6 and the Mach number was 0.6

Table 1. Summary of experimental investigations undertaken by different researchers in different tunnels using a Standard Dynamics Model.

1a. High-speed flows.

Researchers Establishment	**Tunnel Test Section**	**SDM Span (Scale)***	**Velocity Reynolds No. Mach No.**	**Oscillatory Motion**
Cyran (1981) AEDC (USA)	Wind Tunnel 4 foot × 4 foot	502.9 mm (2.200)	$Re/ft = 0.5 \times 10^6$ to $Re/ft = 5.0 \times 10^6$ $M_t = 0.3$ to 1.3	Pitch oscillations $\omega\bar{c}/2V = 0.015$ to 0.055 Yaw oscillations
Coulter & Marquart (1982) AEDC (USA)	Wind Tunnel 4 foot × 4 foot	502.9 mm (2.200)	$Re = 0.62 \times 10^6$ to $Re = 1.56 \times 10^6$ $M_t = 0.3$ to 1.3	Roll oscillations Pitch oscillations $f = 7.5$ Hz Yaw oscillations
Beyers & Moulton (1983) NAE (Canada)	Wind Tunnel 0.75 m × 0.40 m	228.6 mm (1.000)	$Re/m = 10.3 \times 10^6$ $M_t = 0.6$	Roll oscillations
Beyers *et al*. (1984) also see Beyers (1985) NAE (Canada)	Wind Tunnel 0.75 m × 0.40 m	228.6 mm (1.000)	$Re/m = 10.4 \times 10^6$ $M_t = 0.6$	Pitch oscillations $\omega\bar{c}/2V = 0.045$ Yaw oscillations
Jansson & Torngren (1985) FFA (Sweden)	Wind Tunnels 0.7 m² 0.8 m²	290 mm (1.269)	$Re = 1.0 \times 10^6$ $M_t = 0.6$ to 1.05	Pitch oscillations $\omega\bar{c}/2V = 0.008$ to 0.02 Yaw oscillations
Schmidt (1985) DFVLR (Germany)	Wind Tunnel 1 m × 1 m	344.89 mm (1.509)	$Re = 1.03 \times 10^6$ to $Re = 1.54 \times 10^6$ $M_t = 0.60$ to 1.20	Roll oscillations Pitch oscillations $\omega\bar{c}/V = 0.015$ to 0.040 Yaw oscillations
Kabin *et al*. (1995) Russia	Wind Tunnels 2.75 m × 2.75 m 1.0 m × 1.0 m	360 mm (1.575)	$M_t = 0.60$	Roll oscillations Pitch oscillations $f = 10$ to 25 Hz Yaw oscillations
Ueno & Miwa (2001) (NAL) Japan	Wind Tunnel 2 m × 2 m	701.4 mm (3.068)	$Re = 2.31 \times 10^6$ to $Re = 2.95 \times 10^6$ $M_t = 0.6$ to 1.05	Roll oscillations Pitch oscillations $\omega\bar{c}/2V = 0.015$ to 0.027 Yaw oscillations

1b. Low-speed flows.

Researchers Establishment	**Tunnel Test Section**	**SDM Span (Scale)***	**Velocity Reynolds No. Mach No.**	**Oscillatory Motion**
Huang & Beyers (1990) NAE (Canada)	Wind Tunnel 2.74 m × 1.93 m	228.6 mm (1.000)	$V = 69, 100$ m/s $Re = 3.9 \times 10^5$ $Re = 5.7 \times 10^5$	Model stationary
Guglieri & Quagliotti (1991) TPI/TU (Italy)	Wind Tunnel 3.0 m (diam)	609 mm (2.664)	$Re = 4.0 \times 10^5$ $Re = 6.6 \times 10^5$ $M_t \approx 0.1$	Roll oscillations Pitch oscillations $\omega\bar{c}/2V = 0.016, 0.046$ Yaw oscillations
Alemdaroglu *et al*. (2001) Middle East Technical University (Turkey)	Wind Tunnel 10 foot × 8 foot	609 mm 2.664	$V = 20$ m/s $V = 30$ m/s $V = 40$ m/s	Pitch oscillations $\omega\bar{c}/2V = 0.046$
Erm (Present study) DSTO (Australia)	Water Tunnel	228.6 mm (1.000)	$Re \approx 8590$ $V = 0.1$ m/s	Pitch oscillations $\omega\bar{c}/2V = 0.05$

* Scale relative to DSTO SDM.

Non-dimensional frequencies of oscillation, $\omega b/2V$, were 0.016 and 0.027, and the oscillation amplitudes, $\Delta\alpha$, were ±1.0° and ±1.5°. The researchers measured force and moment coefficients, C_Y, C_Z, C_l, C_m and C_n, for values of α varying between -1.2° and +41.3° and β varying between -5° and +5°. They also measured static derivatives, $C_{Y\beta}\sin\alpha$, $C_{Z\beta}\sin\alpha$, $C_{l\beta}\sin\alpha$, $C_{m\beta}\sin\alpha$, and $C_{n\beta}\sin\alpha$, as well as direct, cross and cross-coupled combined dynamic derivatives, for the same ranges of α and β.

Beyers, Kapoor & Moulton (1984) (also see Beyers, 1985) carried out experiments with a SDM in the NAE 0.75 m by 0.40 m Dynamics Wind Tunnel. Their SDM had a wing span, b, of 228.6 mm and a MAC, $\bar{c}$, of 86.2 mm. They developed a special rig to enable the model to be subjected to forced oscillations in both pitch and yaw. The test Reynolds number per metre was 10.4×10^6 and the Mach number was 0.6. For the pitch oscillations, α was varied in steps from 0° to 40°, β was set at 0° and 5°, the reduced frequency, $\omega\bar{c}/2V$, was 0.045, and the amplitude of the oscillations, $\Delta\alpha$, was ±1.0°. For the yaw oscillations, α was varied in steps from 0° to 30°, β was set at 0° and 5°, the reduced frequency, $\omega b/2V$, was 0.117, and the amplitude of the oscillations, $\Delta\beta$, was ±1.0°. The researchers measured a wide range of aerodynamic data, including force and moment coefficients, C_Y, C_Z, C_l, C_m and C_n, direct, cross and cross-coupled static derivatives, $C_{l\alpha}$, $C_{m\alpha}$, $C_{n\alpha}$, $C_{l\beta}\cos\alpha$, $C_{m\beta}\cos\alpha$, $C_{n\beta}\cos\alpha$, C_{l_q}, C_{m_q} and C_{n_q}, combined direct dynamic derivatives, $C_{m_q}+C_{m_{\dot{\alpha}}}$ and $C_{n_r}+C_{n_{\dot{\beta}}}$, as well as combined cross and cross-coupled dynamic derivatives.

Jansson & Torngren (1985), from the Aeronautical Research Institute of Sweden (FFA), conducted tests with a SDM, having a wing span of 290 mm, in two high-speed wind tunnels, having cross-sectional areas of 0.7 and 0.8 m^2. The model was tested at Mach numbers within the range 0.6 to 1.05, for a Reynolds number of 1×10^6. The model was subjected to pitching and yawing oscillations, as well as continuous rolling. For the pitching oscillations, the model was oscillated at reduced frequencies, $\omega\bar{c}/2V$, of 0.008, 0.014, 0.019 and 0.020. Pitching-moment derivatives, $C_{m\alpha}$ and $C_{m_q}+C_{m_{\dot{\alpha}}}$, were measured, as well as a wide range of other derivatives.

Schmidt (1985) undertook a comprehensive testing program in the DFVFR (Deutsche Forschungs- und Versuchsanstalt fur Luft- und Raumfahrt) transonic wind tunnel using a SDM having a span of 344.89 mm. The model was subjected to forced oscillations in roll, pitch and yaw. Tests were done at Mach numbers within range 0.6 to 1.2, and the majority of the measurements were taken for a Reynolds number of 1.03×10^6 (based on MAC). Angles of attack varied between 0° and 30° (approximate range), and the excitation frequencies varied from 2 to 20 Hz. A wide range of aerodynamic coefficients and static and dynamic derivatives, corresponding to the roll, pitch and yaw oscillations, were obtained.

Kabin *et al*. (1995) undertook a testing program using a SDM in a large transonic wind tunnel and a small high-speed wind tunnel at the Central Aerohydrodynamic Institute in Russia – the tunnels had dimensions of 2.75 m by 2.75 m and 1.0 m by 1.0 m respectively. Their SDM, which had a wing span of 360 mm, was mounted on a rig with elastic elements and independently subjected to free oscillations in roll, pitch and yaw. The oscillations were imparted to the model using a special device. The model was tested at a Mach

number of 0.6, the amplitude of the oscillations (roll, pitch and yaw) did not exceed ±2.5° and the frequency of oscillation (roll, pitch and yaw) was within the range 10 to 25 Hz. Kabin *et al*. measured stiffness derivatives, C_{Z_α} and C_{m_α}, damping derivatives, $C_{Z_q}+C_{Z_{\dot\alpha}}$ and $C_{m_q}+C_{m_{\dot\alpha}}$, as well as static and dynamic derivatives for roll and yaw.

Ueno & Miwa (2001) conducted tests using a SDM in the 2 m by 2 m transonic wind tunnel at the National Aerospace Laboratory (NAL), Japan. Their SDM had a wing span, b, of 701.4 mm and a MAC, $\bar{c}$, of 265 mm, and was subjected to forced oscillations in roll, pitch and yaw, at oscillation amplitudes of either ±1° or ±3°. Tests were done at Reynolds numbers varying from 2.31×10^6 to 2.95×10^6 (based on MAC), and Mach numbers varying from 0.6 to 1.05. Reduced frequencies of oscillation, $k = \omega\bar{c}/V$, varied from 0.03 to 0.053 ($k = \omega\bar{c}/2V$ varied from 0.015 to 0.027 respectively). Tests were done for angles of attack ranging from 0° to 20°. The researchers measured a wide range of roll, pitch and yaw parameters, including static coefficients and static and dynamic derivatives.

5.2 Low-Speed Flows

Huang & Beyers (1990) carried out tests with a SDM, having a wing span of 228.6 mm, in the NAE 2.74 m by 1.93 m low-speed wind tunnel. Static force and moment coefficients, C_Y, C_Z, C_l, C_m and C_n, were measured using a six-component strain-gauge balance. All tests were done with the model stationary. Tests were done for free-stream velocities of 69 and 100 m/s, corresponding to Reynolds numbers of 3.9×10^5 and 5.7×10^5 respectively. Data were acquired for α varying from 0° to 90°, in 2° increments, for $\beta = 0°$.

Guglieri & Quagliotti (1991) (see also Guglieri & Quagliotti, 1993) carried out experiments with a SDM in the low-speed wind tunnel at the Turin Polytechnic Institute/Technical University (Italy) (TPI/TU). The tunnel has a circular test section of diameter 3.0 m. Their SDM, which had a wing span, b, of 609 mm and a MAC, $\bar{c}$, of 220 mm, was mounted on a five-component strain-gauge balance and attached to a specially-designed rig that enabled the model to be oscillated independently in roll, pitch or yaw. The model was tested at Reynolds numbers of 4.0×10^5 and 6.6×10^5 (based on MAC), at angles of attack up to 60° and angles of sideslip up to 10°. For the rolling oscillations, the reduced frequencies of oscillation, $\omega b/2V$, were 0.076 and 0.255, and the amplitudes of the oscillations were ±1.6° and ±2.1°. For the pitching oscillations, the reduced frequencies, $\omega\bar{c}/2V$, were 0.016 and 0.046, and the amplitudes were ±0.5° and ±3.0°. For the yawing oscillations, the reduced frequencies, $\omega b/2V$, were 0.061 and 0.102, and the amplitudes were ±0.5° and ±1.5°. Guglieri & Quagliotti measured force and moment coefficients, C_Y, C_Z, C_l, C_m and C_n, static derivatives, C_{m_α}, $C_{l_{\dot\beta}}$, and $C_{n_{\dot\beta}}$, as well as direct combined dynamic derivatives, $C_{m_q}+C_{m_{\dot\alpha}}$, $C_{l_p}+C_{l_{\dot\beta}}\sin\alpha$ and $C_{n_r}+C_{n_{\dot\beta}}$, for different values of α. They indicated that their experimental results were generally in good agreement with those of Huang & Beyers (1990), Beyers & Moulton (1983), Beyers, Kapoor & Moulton (1984), Torngren (1985) and Schmidt (1985), taking into account the different characteristics of the wind tunnels and the model suspensions between the different investigations.

Alemdaroglu *et al*. (2001) (see also Alemdaroglu *et al*., 2002, Altun & Iyigun, 2004) carried out tests with a SDM in the 10 foot by 8 foot low-speed wind tunnel at the Middle East Technical University, Ankara, Turkey. Their SDM had a wing span, b, of 609 mm and a MAC, $\bar{c}$, of 220 mm. It was mounted on a five-component strain-gauge balance and attached to a special rig that could be used to oscillate the model with simple harmonic motion in the pitch plane, with the model set at different angles of sideslip. The test velocities used were 20 m/s, 30 m/s and 40 m/s. Tests were done for values of α varying between –6° and 30°, for β set at 0°. The non-dimensional frequency of oscillation, $\omega\bar{c}/2V$, was 0.046 and the oscillation amplitude was ±1° and ±2°. The researchers measured static force and moment coefficients, C_Z, C_l and C_m, stiffness derivatives, $C_{Z\alpha}$, $C_{l\alpha}$ and $C_{m\alpha}$, as well as damping derivatives, $C_{Zq}+C_{Z\dot{\alpha}}$, $C_{lq}+C_{l\dot{\alpha}}$ and $C_{mq}+C_{m\dot{\alpha}}$. They found that their experimental data showed good agreement with those obtained in other facilities, NAE and TPI/TU. For the dynamic tests, static and dynamic derivatives were found to exhibit highly non-linear behaviour. They indicated that data were affected by the tunnel flow characteristics and the model support system. They stated that experimental test rigs for this type of work are usually massive, which causes large flow-blockage effects near or above the model. This in turn causes artificial pressure fields on the model which result in vortex bursting on the model.

It can be seen from Tables 1a and b that all previous experimental studies using a SDM to measure static and dynamic aerodynamic derivatives have been carried out in wind tunnels, rather than water tunnels. SDMs of different sizes have been used, with wing spans ranging from 228.6 mm to 701.4 mm. Experimental data have been acquired at moderate to high Mach numbers as well as at low Mach numbers. There is 2 or 3 orders of magnitude difference between test Reynolds numbers reported in the literature and that for the current water-tunnel experiments. As well as large variations in Reynolds numbers and Mach numbers for the different investigations, there are also marked differences in oscillation frequencies, free-stream flow non uniformities, rig designs, shock-wave systems and tunnel blockages. For all of the investigations, motion was imparted to the SDM using the forced-oscillation technique, except for the investigation by Kabin *et al*. (1995), who used the free-oscillation technique. It is noteworthy that measured dynamic derivatives given by researchers have been combined derivatives, such as $C_{mq}+C_{m\dot{\alpha}}$, rather than separated derivatives, such as C_{mq} and $C_{m\dot{\alpha}}$. Selected data from some of the investigations are given in Section 7, where they are used as a basis for comparison with the current water-tunnel data.

6. Details of Current Experiments

An experimental program was developed to measure parameters in the DSTO water tunnel, comprising coefficients C_Z and C_m, static (stiffness) derivatives $C_{Z\alpha}$ and $C_{m\alpha}$, and dynamic (damping) derivatives $C_{Zq}+C_{Z\dot{\alpha}}$, $C_{mq}+C_{m\dot{\alpha}}$, C_{Zq}, $C_{Z\dot{\alpha}}$, C_{mq} and $C_{m\dot{\alpha}}$.

6.1 SDM Set-Up When Testing

6.1.1 Static Tests

To measure coefficients C_Z and C_m, experiments were carried out with the SDM not mounted on a sting extension, as shown in Figure 9a. Data were sampled with the model stationary at different values of α.

6.1.2 Dynamic Tests

Derivatives $C_{Z\alpha}$, $C_{m\alpha}$, $C_{Zq}+C_{Z\dot{\alpha}}$ and $C_{mq}+C_{m\dot{\alpha}}$ were also measured using the set-up shown in Figure 9a, but to measure derivatives C_{Zq}, $C_{Z\dot{\alpha}}$, C_{mq} and $C_{m\dot{\alpha}}$, additional experiments were carried out with the SDM mounted on a sting extension, as shown in Figure 9b for a 300 mm extension. Data were sampled with the model oscillating in pitch with simple harmonic motion at different values of α, with the roll and yaw angles fixed at 0°.

6.2 Determination of Offsets in Reference Locations

Ideally, with the SDM not mounted on a sting extension, reference locations comprising (1) the centre of rotation of the dynamic-rig motion system, (2) the SDM datum and (3) the balance calibration reference centre, should all be coincident. However, in practice, small offsets exist between the different reference locations and these offsets have to be accounted for when processing data.

6.2.1 Determination of Offset l_b

Offset l_b, the displacement of the SDM datum forward of the balance calibration reference centre, was determined by carrying out physical metrological measurements when the SDM was mounted on the balance. Offset l_b was found to be -0.59 mm, indicating that the balance calibration reference centre is slightly upstream of the SDM datum.

6.2.2 Determination of Offset l_c

Offset l_c, the displacement of the SDM datum forward of the centre of rotation of the dynamic-rig motion system, was determined by first attaching 2 fluorescent registration markers (diameter of markers = 3 mm) to the SDM (see Figure 1) and videoing the movement of the markers as the SDM was oscillated in simple harmonic motion in pitch by ±22° about a mean pitch angle of 22° for the case when no sting extension was used. Special software was then used to interrogate the video recording to extract a set of coordinates for the centres of each of the markers, and these coordinates were then curve fitted to determine the location of the centre of rotation of the dynamic-rig motion system relative to the markers. Figure 10 shows the locations of the registration markers and the fitted circles. Since the values of the extracted locations of the registration markers are based on an arbitrary origin chosen by the video operator, the locations have therefore been adjusted and plotted so that the zero points on the axes correspond to the centre of

rotation of the rig, as shown in Figure 10. The sum of the distances from the centre of rotation to the centres of each of the markers, as determined from the fitted circles, is 129.78 + 70.426 = 200.206 mm. However, the distance between the centres of the markers determined by carrying out physical metrological measurements was found to be 199.84 mm. The reason for the discrepancy is that the centres of the markers and the centre of rotation of the dynamic-rig motion system are not collinear when projected onto a vertical plane. It was found that the centre of rotation of the rig is offset 5.8 mm in the z direction and 0.28 mm in the x direction from the SDM datum. Thus, for the case of no sting extension, offset l_c is equal to -0.28 mm, indicating that the SDM datum is slightly downstream of the centre of rotation of the dynamic-rig motion system. The offset in the z direction has negligible effect on the values of the measured parameters.

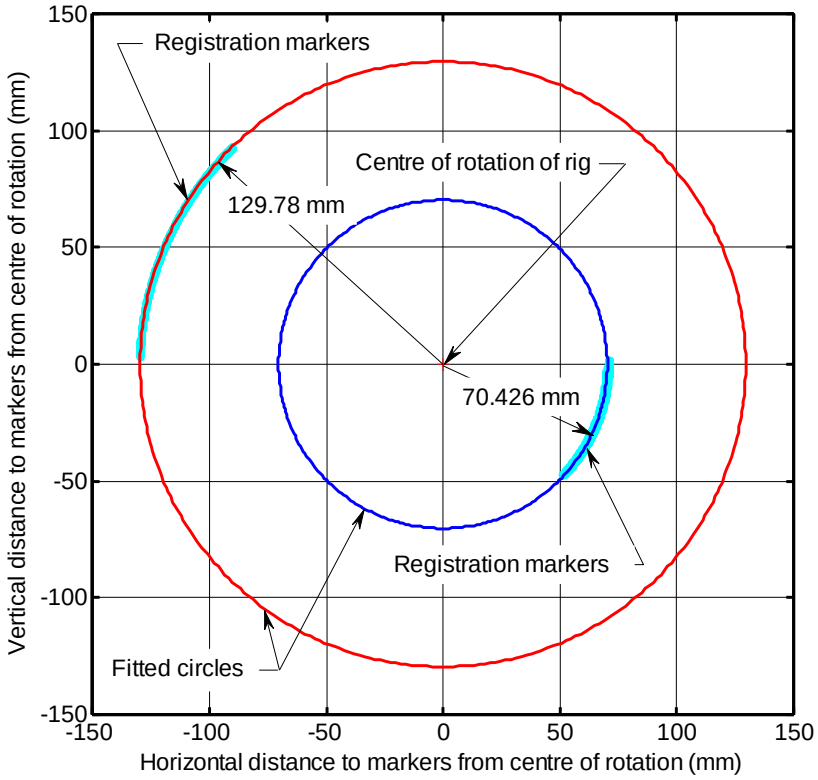

Figure 10. Location of centres of registration markers, obtained from a video recording, plus superimposed fitted circles.

6.3 Use of Roof on Test Section

Prior to starting the main test program, preliminary tests with the model oscillating were conducted to investigate the quality of the sampled voltage signals from the normal-force and pitching-moment channels on the two-component strain-gauge balance. Initially measurements were made with no roof on the water surface in the test section. Sampled voltages, corrected for the effects of tare voltages (see Sections 6.5.3 and 6.6.3), for the

normal-force and the pitching-moment channels are shown in Figures 11a and 12a respectively (blue curves). As can be seen, the voltages signals for the two cases are unacceptably noisy. Power spectral densities were computed for both of these (blue) voltage signals, and these are shown in Figures 11c and 12c (blue spectra). In both cases, there were unexpected and unwanted spectral peaks in the vicinity of 1 Hz. The cause of these spectral peaks had to be eliminated before the main testing program could be started. An inspection of the water surface while the tunnel was running at a free-stream velocity of 0.1 m/s (nominal value) revealed that there were small perturbations in the level of the water surface, as a consequence of the flow through the test section. In an attempt to alleviate the problem, a Perspex roof was suspended above the test section so that it just touched the water surface, without causing any blockage to the oncoming flow. With the roof in place, there were no observable perturbations in the level of the water surface. Voltages were resampled and corrected for the effects of tare as previously and spectra were once again computed. For this case, the sampled voltages for the normal-force and the pitching-moment channels are shown in Figures 11b and 12b respectively (red curves) and corresponding spectra are shown in Figures 11c and 12c (red spectra). As can be seen, the voltage signals are less noisy when a roof is used and the peaks in the spectra at about 1 Hz have been eliminated. Spectral peaks at about 0.045 Hz, corresponding to the frequency of the sinusoidal oscillations of the model, are clearly shown on the spectra. As a consequence of the above findings, the main testing program was carried out with a roof on the test section.

6.4 Test Matrices

6.4.1 Static Tests

The test matrix used when measuring force and moment coefficients is shown in Table 2.

Table 2. Matrix of static tests.

Sting Extension l_c (mm)	**Pitch Angles θ (deg)**	**Reduced Frequency ($k = \omega\bar{C}/2V$)**	**Free-Stream Velocity V (m/s)**	**Oscillation Frequency f (Hz)**	**Oscillation Amplitude $\Delta\theta$ (deg)**
0.0	-4° to 30°, 1° increments	0.0	0.10	0.0	±0.0

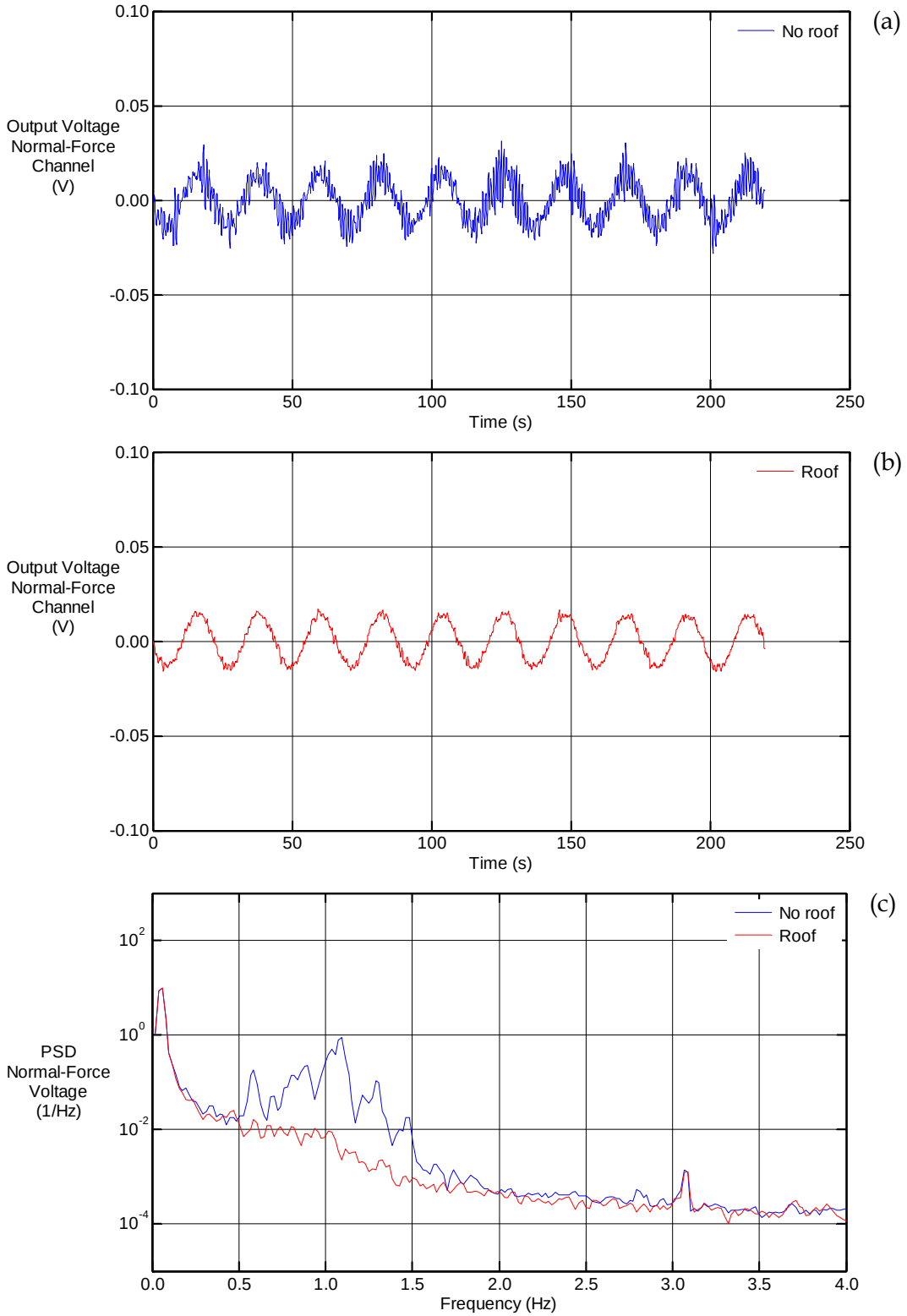

Figure 11. Data from preliminary tests, (a) voltage signal from the normal-force channel without the roof on the test section, (b) voltage signal from the normal-force channel with the roof on the test section, (c) spectra for voltage signals for both the no-roof and the roof cases.

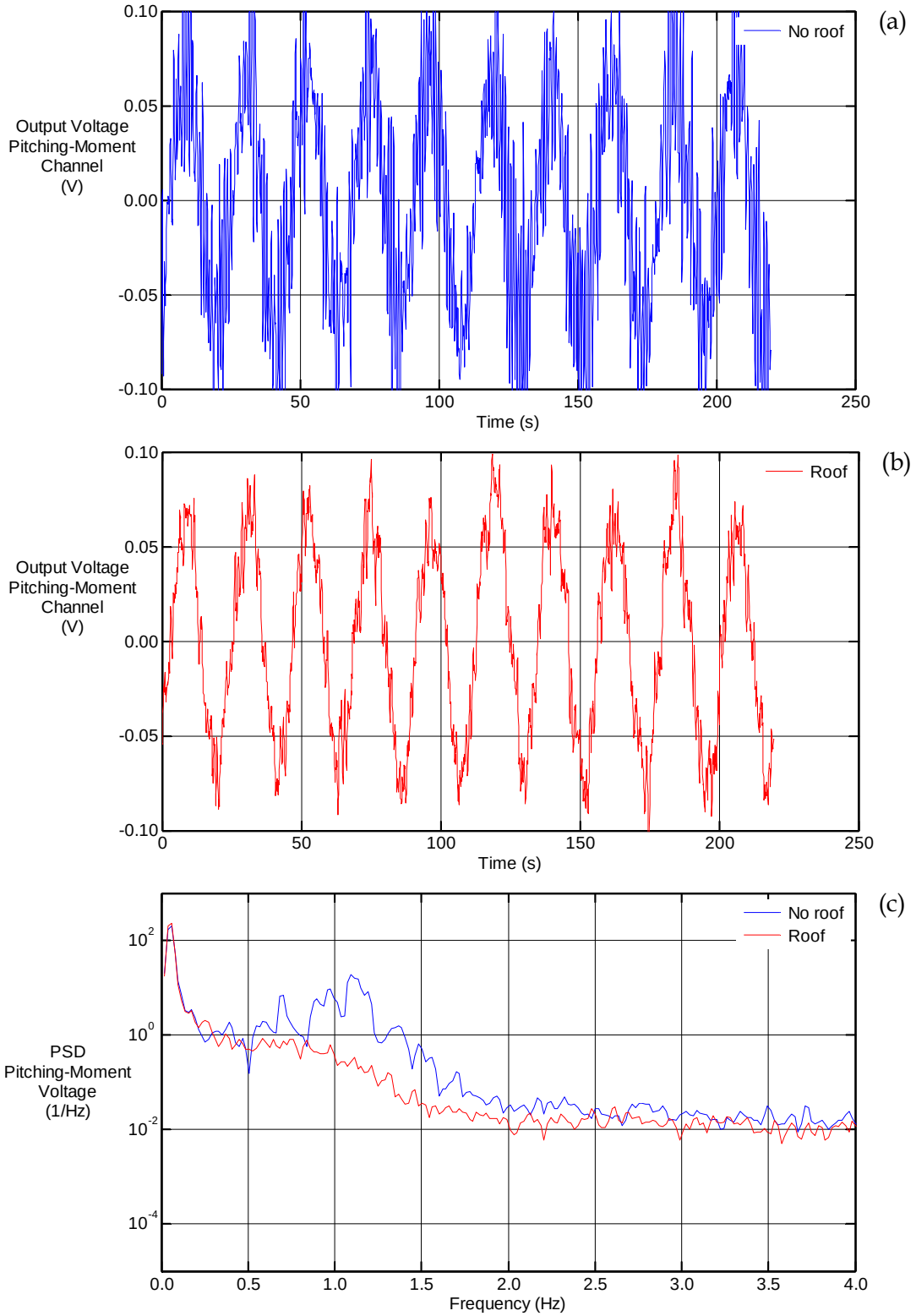

Figure 12. Data from preliminary tests, (a) voltage signal from the pitching-moment channel without the roof on the test section, (b) voltage signal from the pitching-moment channel with the roof on the test section, (c) spectra for voltage signals for both the no-roof and the roof cases.

6.4.2 Dynamic Tests

The test matrix used when measuring longitudinal static and dynamic derivatives is shown in Table 3. Using two sting extensions, data were acquired for the same pitch angles, nominal reduced frequencies, nominal free-stream velocities, oscillation frequencies and oscillation amplitudes.

Table 3. Matrix for dynamic tests.

Sting Extension l_c (mm)	**Pitch Angles θ (deg)**	**Reduced Frequency ($k = \omega\bar{C}/2V$)**	**Free-Stream Velocity V (m/s)**	**Oscillation Frequency f (Hz)**	**Oscillation Amplitude $\Delta\theta$ (deg)**
0.0	0° to 30°, 2° increments	0.05	0.10	0.018463	±0.5
300.0	0° to 30°, 2° increments	0.05	0.10	0.018463	±0.5

It is important to note that the selected free-stream velocity, V = 0.1 m/s, given in Tables 2 and 3, and oscillation frequency, f = 0.018463 Hz, given in Table 3, are in fact nominal values. To preserve flow similarity over a model during a testing program, it is important that all tests were carried out at the same Reynolds number. Since the temperature of the water in the tunnel could vary markedly from day-to-day during the testing program, the kinematic viscosity of the water also changed markedly, and this affected the Reynolds number. The free-stream velocity used for the tests therefore had to be adjusted to maintain a constant Reynolds number for the different water temperatures. The free-stream velocity and oscillation frequency shown in the tables were computed for a water temperature of 20° C, corresponding to a Reynolds number of about 8590. The temperature of the water in the tunnel varied from about 11° C (winter) to about 27° C (summer). To maintain a constant Reynolds number of 8590 when testing at these two temperatures, the free-stream velocity had to be set between V = 0.127 m/s for 11° C and V = 0.085 m/s for 27° C. The oscillation frequency, f, had to be adjusted accordingly to maintain the reduced frequency, k, at a value of 0.05 for all temperatures.

6.5 Procedure Used For Static Experiments

6.5.1 Setting of Gains and Cut-Off Frequencies

The amplifier gains and the filter cut-off frequencies used in the tests were set using the GUI for the Bridge-Conditioner Unit (BCU) shown in Figure 5. The gain for the normal-force (Z) channel was set at 620 and the gain for the pitching-moment (M) channel was set at 1240. The low-pass analog filters in the BCU were set at 1 Hz.

6.5.2 Control of Model Pitch Angle, Free-Stream Velocity and Data Sampling

The model pitch angle, tunnel free-stream velocity and data sampling were all controlled using the GUI shown in Figure 8. For the static tests to measure coefficients, the pitch angle was varied from -4° to 30° in 1° increments. Instantaneous values of free-stream velocity, model pitch angle, water temperature and bridge output voltages were sampled at 5 Hz for 60 s for each pitch-angle setting and were written to a data file on the disk of the PC for subsequent analysis. Thus $60 \times 5 = 300$ samples of each parameter were acquired for each pitch angle. Once sampling had started, it was continuous from the start of the profile to the end, which meant that data were sampled even when the model was in motion between the different settings of pitch angle. When processing experimental data to determine coefficients, only data points sampled while the model was stationary were used (see Section 6.5.4).

6.5.3 Tare Runs

For the model positioned at the different pitch angles, there were contributions to the measured forces and moments from two different sources, namely

(1) the variation of the model weight and buoyancy with pitch angle,
(2) the aerodynamic flow-induced forces and moments on the model due to water flowing over the model.

To isolate the desired aerodynamic loads, item (2), it was necessary to measure the forces and moments due to (1) by carrying out tare runs with the water not flowing, and then to subtract these tare loads from the combined loads measured with the water flowing. The sampling parameters (filter settings, number of samples, sampling frequency) used for the tare runs, i.e. water not flowing, were identical to those used when the water was flowing. Tare runs were done both directly before, and directly after, measuring flow-induced loads on the model. This was done to take account of the fact that the output voltages from the strain-gauge balance may have drifted between the start and end of an experimental run. Drifting of output voltages was assumed to be linear.

6.5.4 Processing of Experimental Data

Coefficients, C_Z and C_m, associated with a stationary SDM, were processed in the conventional manner. Sampled voltages from the strain-gauge balance were converted to normal forces and pitching moments using the balance calibration relationships. The data were corrected for the effects of tare, as described above. The normal forces and pitching moments were then converted to coefficients. Although 300 sets of data were sampled for each setting of the pitch angle of the model, only 125 sets of data, acquired towards the end of the sampling period for each setting, were averaged to determine mean values of coefficients. The earlier sets of data at each setting were discarded since flow transients may have still been present as a consequence of the model moving to a new setting.

6.6 Procedure Used For Dynamic Experiments

6.6.1 Setting of Gains and Cut-Off Frequencies

The settings used for the gains and filter cut-off frequencies for the dynamic experiments were the same as those used for the static experiments.

6.6.2 Control of Model Pitch Angle, Free-Stream Velocity and Data Sampling

As for the static tests, the model pitch angle, tunnel free-stream velocity and data sampling were all controlled using the GUI shown in Figure 8. The model was also "homed" and the strain-gauge balance nulled as previously.

For the dynamic tests to measure derivatives, the model was oscillated in pitch with simple harmonic motion within the range ±0.5° about mean pitch angles varying from 0° to 30° in 2° increments. The reduced frequency, $k = \omega\bar{c}\,/2V$ was 0.05. Instantaneous values of free-stream velocity, model pitch angle, water temperature and bridge output voltages were sampled at 10 Hz for 15 cycles and were written to a data file on the disk of the PC for subsequent processing. For a free-stream velocity of 0.1 m/s and a reduced frequency of 0.05, a cycle took typically about 54 s to complete. Although data were sampled for 15 cycles, data for the initial cycles, where starting transients were present, were disregarded when determining aerodynamic derivatives.

When carrying out dynamic tests, the amplitude of the oscillations was chosen to be as small as practically possible to minimise the effects of non-linearities in the model's aerodynamic characteristics. Obviously compromises had to be made in the experimental program due to practical considerations, i.e. it was pointless choosing an oscillation amplitude that was so small that the variations in parameters throughout a cycle were too small to measure accurately. The amplitude chosen for the current tests, i.e. ±0.5°, was thought to be a good compromise.

6.6.3 Tare Runs

As for the static tests, tare runs also had to be done for the dynamic tests. The procedure used to carry out tare runs for the dynamic tests was similar to that used for the static case, described above, except of course in the dynamic case the tare runs were done with the model oscillating sinusoidally in pitch with the water not flowing.

For the dynamic tests, the inertial forces and moments on the model due to its motion were assumed to be very small for the pitching oscillations used for the current tests (period typically about 54 s) and could therefore be neglected. The assumption of very small inertia loads for models oscillated at low frequency in water was based on the findings of Suárez & Malcolm (1995). They subjected models of a 70° delta wing and an F/A-18 aircraft to oscillations in pitch in stationary water and measured the normal forces on the models. They found that the loads were very small, being only about 1% of their values when the models were oscillating with water flowing. They also found that similar

results were obtained when models were oscillated when there was no water in the tunnel. They concluded that the resistance of the surrounding water being displaced by the moving models had no major effect on the measured loads.

6.6.4 Processing of Experimental Data

Instantaneous coefficients, C_Z and C_m, associated with an oscillating SDM, were processed in the conventional manner. Sampled voltages from the strain-gauge balance were converted to normal forces and pitching moments using the balance calibration relationships. The data were corrected for the effects of tare, as described above. The normal forces and pitching moments were then converted to coefficients.

Static and dynamic aerodynamic derivatives, $C_{Z\alpha}$, $C_{m\alpha}$, $C_{Zq}+C_{Z\dot{\alpha}}$, $C_{mq}+C_{m\dot{\alpha}}$, C_{Zq}, $C_{Z\dot{\alpha}}$, C_{mq} and $C_{m\dot{\alpha}}$, associated with an oscillating SDM, were computed from measured instantaneous coefficients and angles of attack, as well as from the reduced frequency of oscillation and SDM geometrical parameters, using a Matlab® program developed by Newman (2011) – see Section 4.

7. Analysis of Experimental Results

To assess the goodness of measurements obtained using a SDM in the DSTO water tunnel, it was necessary to compare them with corresponding wind-tunnel measurements, where available, obtained by other researchers, as shown in Figures 13 to 22 for C_Z, C_m, $C_{Z\alpha}$, $C_{m\alpha}$, $C_{Zq}+C_{Z\dot{\alpha}}$, $C_{mq}+C_{m\dot{\alpha}}$, C_{Zq}, $C_{Z\dot{\alpha}}$, C_{mq} and $C_{m\dot{\alpha}}$ respectively.

Although many researchers have carried out tests using the SDM to measure static and dynamic derivatives, there is not a standardised testing schedule. Researchers have conducted tests on SDMs having spans varying from 228.6 mm to 701.4 mm. Tunnel operating conditions have varied from high-velocity flows, having Mach numbers up to 1.3, down to low-velocity flows of 20 m/s. Reduced frequencies of oscillation and oscillation amplitudes have also varied for the different testing programs. Each tunnel had its own unique dynamic-rig configuration, used to oscillate an SDM. These rigs were often quite substantial, resulting in significant tunnel blockages, which varied from tunnel to tunnel, affecting the quality of the flow around SDMs in different ways. All of the above differences in the testing programs inevitably led to variations in acquired data for the different cases. The tests were highly specialised and there is no definitive data set to be used for comparison purposes.

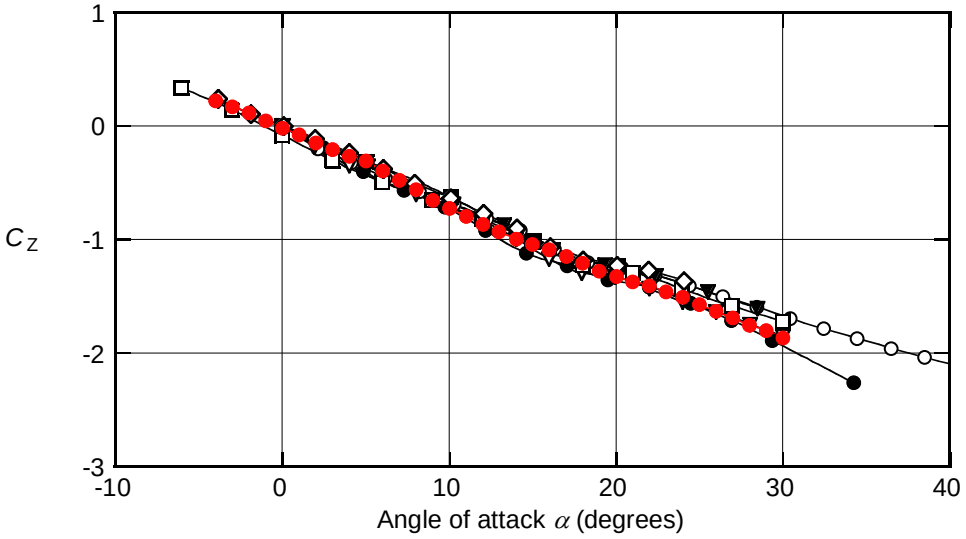

Figure 13. C_Z vs. α for different investigations.

◇ *Cyran (1981), M_t = 0.6;* ● *Beyers et al. (1984), M_t = 0.6;* ▼ *Schmidt (1985), M_t = 0.6;* ○ *Huang & Beyers (1990), V = 70 m/s;* ▽ *Guglieri & Quagliotti (1991), M_t = 0.1 to 0.2;* ■ *Ueno & Miwa (2001), M_t = 0.6;* □ *Alemdaroglu et al. (2001), V = 40 m/s;* ● *DSTO water tunnel, V = 0.1 m/s.*

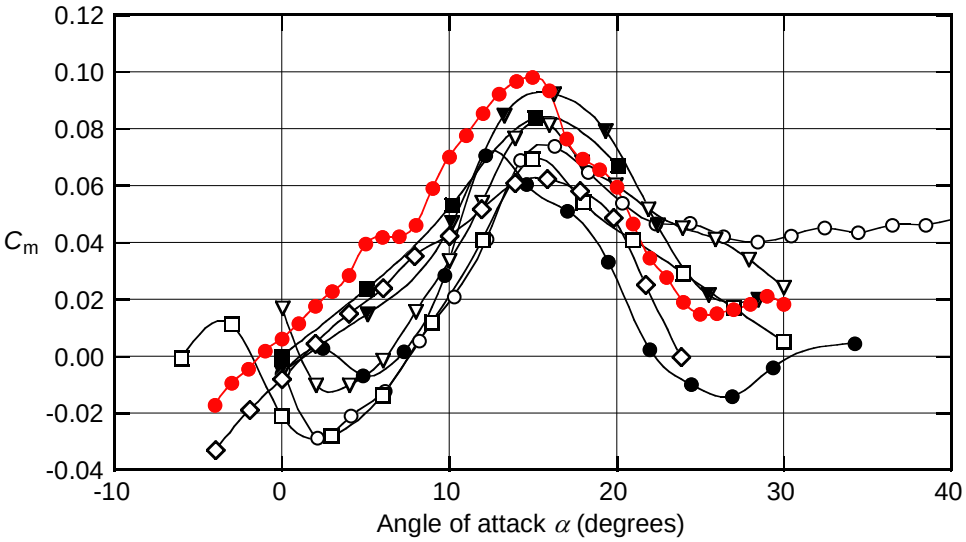

Figure 14. C_m vs. α for different investigations.

◇ *Cyran (1981), M_t = 0.6;* ● *Beyers et al. (1984) (also see Beyers, 1985), M_t = 0.6;* ▼ *Schmidt (1985), M_t = 0.6;* ○ *Huang & Beyers (1990), V = 70 m/s;* ▽ *Guglieri & Quagliotti (1991), M_t = 0.1 to 0.2;* ■ *Ueno & Miwa (2001), M_t = 0.6;* □ *Alemdaroglu et al. (2001), V = 40 m/s;* ● *DSTO water tunnel, V = 0.1 m/s.*

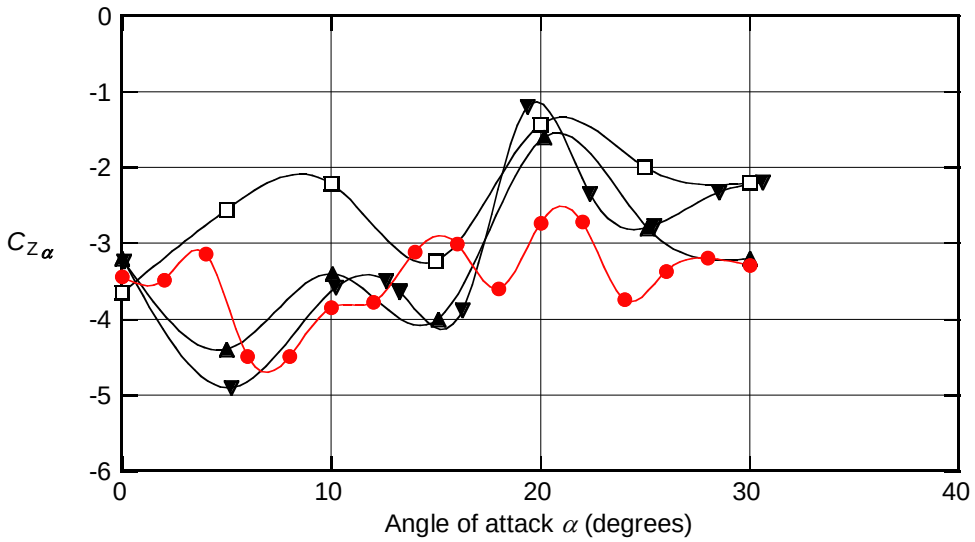

Figure 15. $C_{Z\alpha}$ vs. α for different investigations.

▼ *Schmidt (1985), $M_t = 0.6$;* ▲ *Kabin et al. (1995), $M_t = 0.6$;* □ *Alemdaroglu et al. (2001), V = 30 m/s;* ● *DSTO water tunnel, V = 0.1 m/s.*

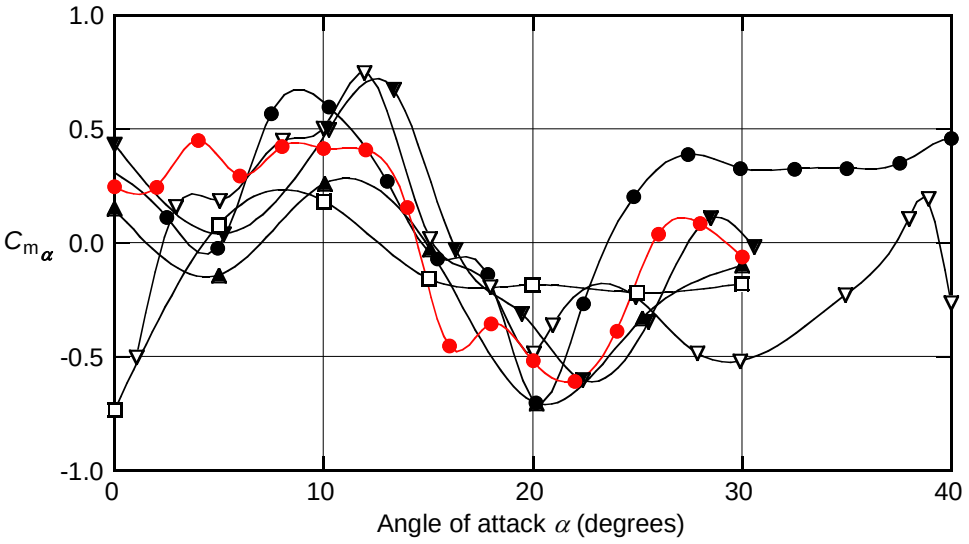

Figure 16. $C_{m\alpha}$ vs. α for different investigations.

● *Beyers et al. (1984) (also see Beyers, 1985), $M_t = 0.6$;* ▼ *Schmidt (1985), $M_t = 0.6$;* ▽ *Guglieri & Quagliotti (1991), $M_t \approx 0.1$;* ▲ *Kabin et al. (1995), $M_t = 0.6$;* □ *Alemdaroglu et al. (2001), V = 30 m/s;* ● *DSTO water tunnel, V = 0.1 m/s.*

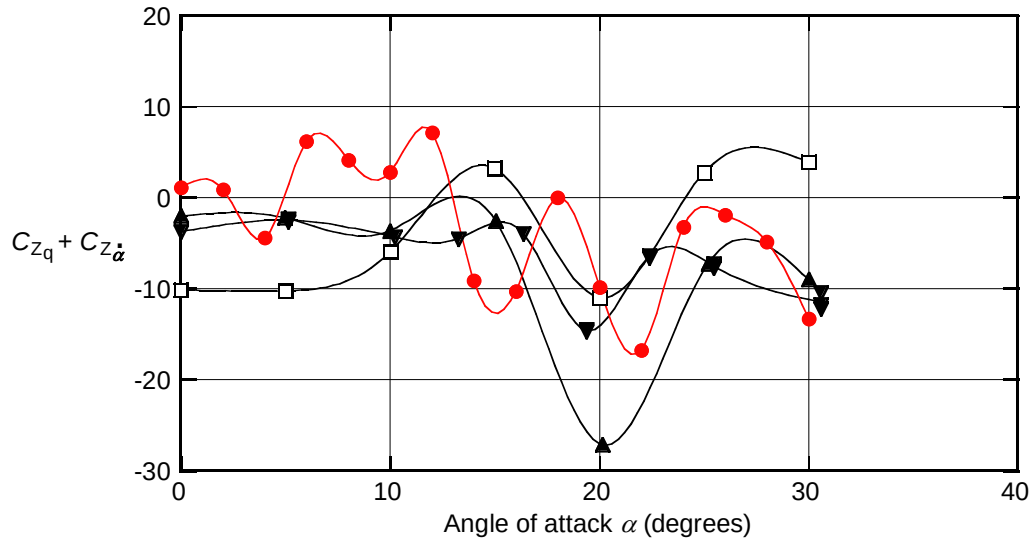

Figure 17. $C_{Z_q} + C_{Z_{\dot{\alpha}}}$ *vs.* α *for different investigations.*

▼ *Schmidt (1985),* $M_t = 0.6$; ▲ *Kabin et al. (1995),* $M_t = 0.6$; □ *Alemdaroglu et al. (2001), V = 30 m/s;* ● *DSTO water tunnel, V = 0.1 m/s.*

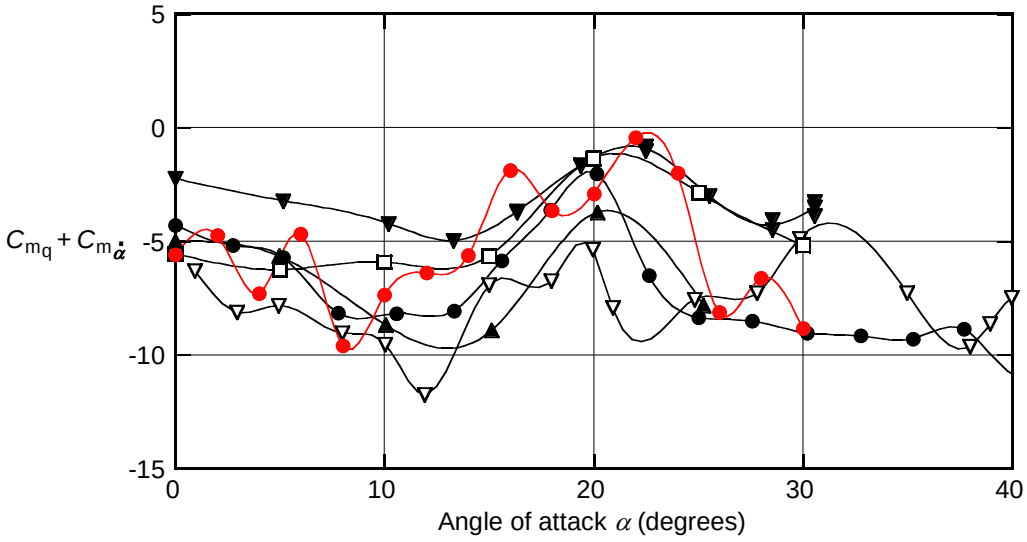

Figure 18. $C_{m_q} + C_{m_{\dot{\alpha}}}$ *vs.* α *for different investigations.*

● *Beyers et al. (1984) (also see Beyers, 1985),* $M_t = 0.6$; ▼ *Schmidt (1985),* $M_t = 0.6$; ▽ *Guglieri & Quagliotti (1991),* $M_t \approx 0.1$; ▲ *Kabin et al. (1995),* $M_t = 0.6$; □ *Alemdaroglu et al. (2001), V = 30 m/s;* ● *DSTO water tunnel, V = 0.1 m/s.*

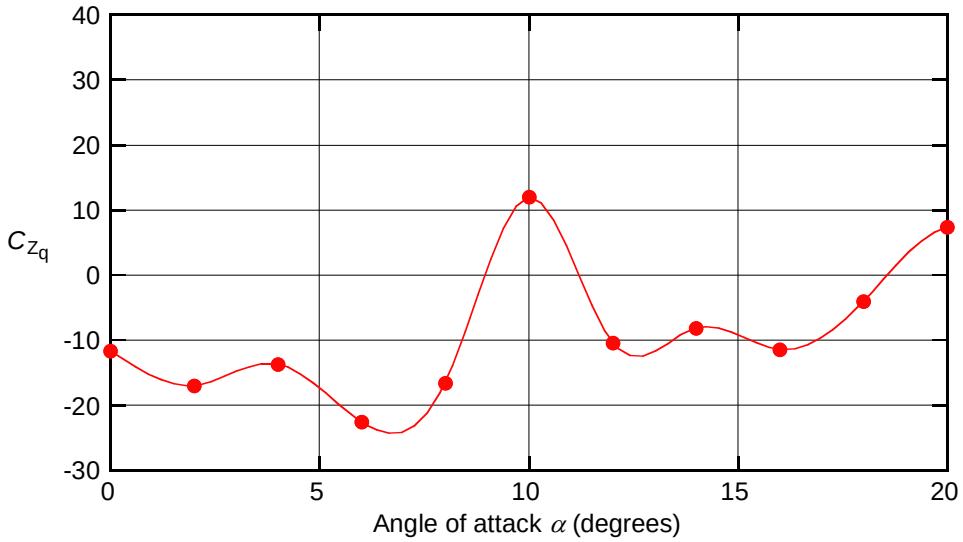

Figure 19. C_{Z_q} *vs.* α. • *DSTO water tunnel.*

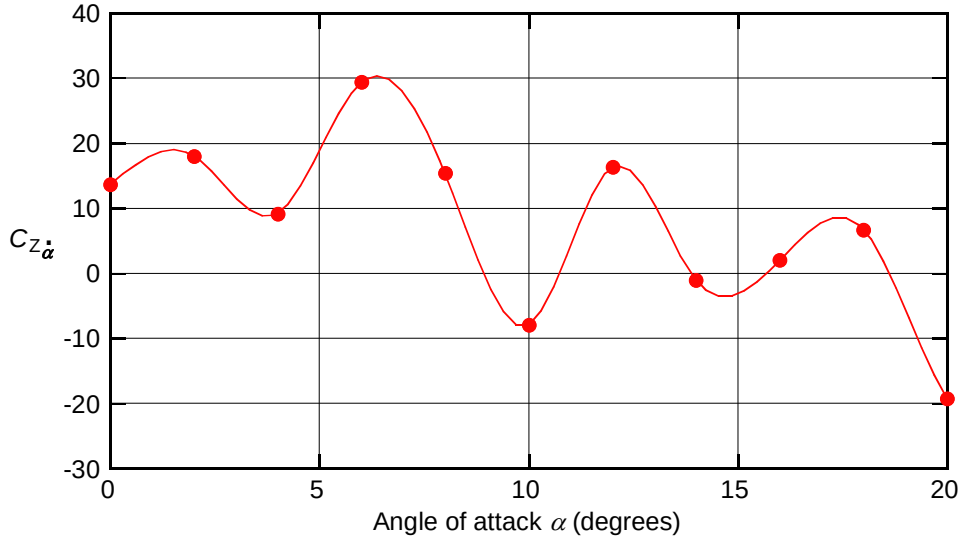

Figure 20. $C_{Z_{\dot{\alpha}}}$ *vs* α. • *DSTO water tunnel.*

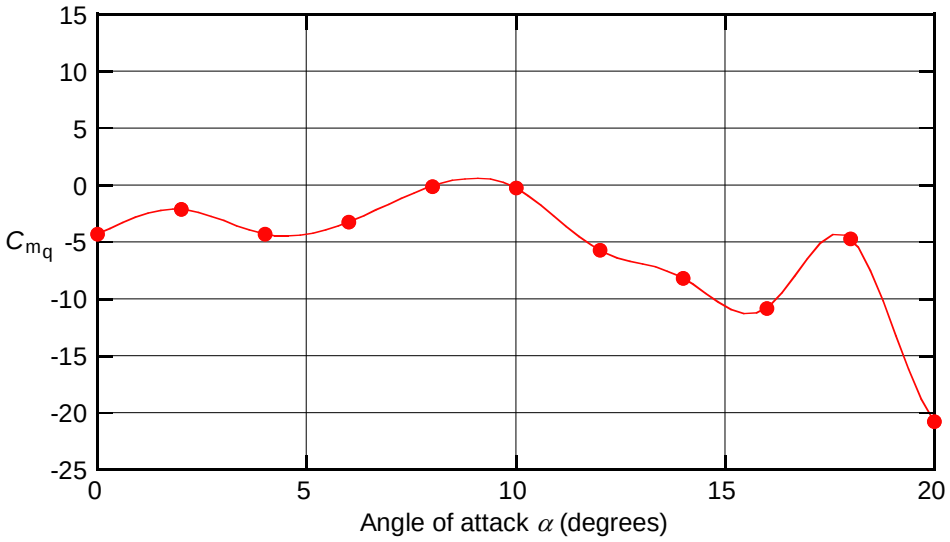

Figure 21. C_{m_q} *vs* α. ● *DSTO water tunnel.*

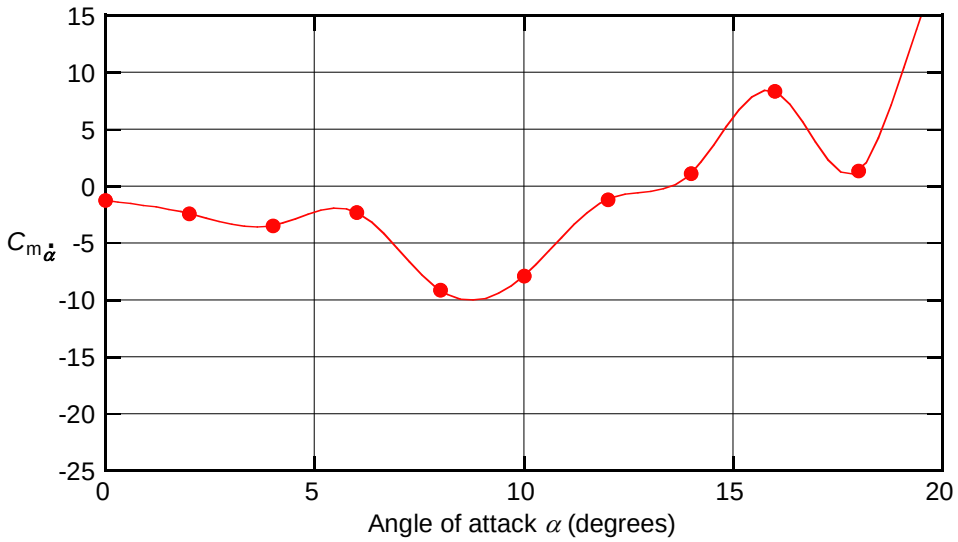

Figure 22. $C_{m_{\dot{\alpha}}}$ *vs* α. ● *DSTO water tunnel.*

Despite the above reservations, and although there are variations in acquired data from the different studies, general trends can be discerned. Plotted water-tunnel SDM data are located within the general scatter of published wind-tunnel data for $M_t \leq 0.6$ and follow the same general trends, giving some credibility to the water-tunnel data. Although wind tunnels are the preferred option to measure derivatives, it is feasible to use a water tunnel to measure derivatives, at least for the SDM, especially if derivatives are required cheaply and quickly

There is a discontinuity in the slope of the C_Z data at $\alpha \approx 18°$, shown in Figure 13, which is consistent with the behaviour found by others. Huang & Beyers (1990) indicate that, due to incremental lift from the strake (leading-edge extension) on the SDM, values of C_Z increase dramatically beyond the value of α corresponding to the wing-alone stall angle, which for the flat surfaces of the SDM is expected to occur at $\alpha \approx 18°$. They further indicate that the aerodynamic characteristics of the model in the range $\alpha = 18°$ to 22° are consistent with the strake vortex bursting over the wing trailing edge. The resulting loss of lift results in the discontinuity in the C_Z curve at $\alpha \approx 18°$.

The water-tunnel C_m data, shown in Figure 14, peak at about the same location as the data of others and follow similar trends. Huang & Beyers (1990) indicate that it appears that separation on the horizontal stabilisers is delayed by downwash from the wings, so that the slope of the curve for the normal force on the stabilisers is kept at relative high values due to the effective lower angle of attack of the flow onto the stabilisers. Thus, when the slope of the normal force *vs* α curve for the wings is reduced by tip stalling above $\alpha = 18°$, a stabilising pitching moment results. The favourable effect of the wing downwash is maintained up to about $\alpha = 30°$, above which the longitudinal stability is lost.

The derivatives are generally highly non-linear with α, which is to be expected, since the complex vortical flow fields over SDMs in tunnels are continuously changing with α, often asymmetrically for tests done with zero sideslip, i.e. $\beta = 0°$. The oscillatory behaviour of the SDM derivative data, shown in Figures 15 to 18, is of some concern. Possible reasons for such behaviour are uncertain, but the behaviour could be due to the fact that the DSTO SDM data were acquired at smaller increments in α than were the wind-tunnel data. The fact that the water-tunnel data follow the same general trends as corresponding wind-tunnel data suggests that the main features of the flow patterns over the water-tunnel SDM are similar to those over the wind-tunnel SDMs. In the absence of surface pressure measurements and images of the flow for the water-tunnel SDM, it is difficult to explain the non-linear behaviour. Values of derivatives measured at DSTO using models such as the SDM were found to be repeatable to typically about 3%.

There does not seem to be any published wind-tunnel data available for separated derivatives, C_{Z_q}, $C_{Z_{\dot{\alpha}}}$, C_{m_q} and $C_{m_{\dot{\alpha}}}$, shown in Figures 19, 20, 21 and 22 respectively, that can be used for comparison purposes with the water-tunnel data. To determine separated derivatives, it is necessary to subject a model to both pitching and plunging motions. The dynamic-testing rigs used by different researchers to determine derivatives for a SDM, referred to in the present report, are not capable of imparting both pitching and plunging motions to models. Typically pitching oscillations about the datum of an aircraft are used

to measure longitudinal dynamic derivatives as a combination of two terms, such as $C_{Zq}+C_{Z\dot{\alpha}}$, while plunging oscillations are used to measure the angle-of-attack-rate term, such as $C_{Z\dot{\alpha}}$ in isolation (see Newman, 2011).

8. Concluding Remarks

The purpose of this investigation was to determine whether it is feasible to measure meaningful static load coefficients and static and dynamic aerodynamic derivatives using a Standard Dynamics Model (SDM) in the DSTO water tunnel. A special load-measurement system and dynamic-testing system, previously developed for the tunnel, was used in the investigation. Static and dynamic tests were carried out at a nominal free-stream velocity of 0.1 m/s. For the static tests, normal-force and pitching-moment coefficients, C_Z and C_m, respectively, were measured for pitch angles varying from -4° to 30° in 1° increments, with the model stationary at each pitch angle. For the dynamic tests, static (stiffness) derivatives, $C_{Z\alpha}$ and $C_{m\alpha}$, and dynamic (damping) derivatives, $C_{Zq}+C_{Z\dot{\alpha}}$, $C_{mq}+C_{m\dot{\alpha}}$, C_{Zq}, $C_{Z\dot{\alpha}}$, C_{mq} and $C_{m\dot{\alpha}}$, were measured by oscillating the model sinusoidally in pitch through an amplitude of ±0.5° at a reduced frequency of 0.05, for mean pitch angles varying from 0° to 30° in 2° increments. When calculating derivatives, data were processed using the methodology developed by Newman (2011). To determine some of the above derivatives, it was necessary to support the model on stings of different lengths.

There are some areas of concern for the water-tunnel investigation to measure derivatives. The water-tunnel SDM was manufactured using stereolithographic techniques and the SDMs used in the wind-tunnel investigations were up to about 3 times as large as the water-tunnel SDM, which most likely means that the water-tunnel model was not manufactured to the same precision as the wind-tunnel models. The flow physics for the SDM in the water tunnel may not be representative of the flow physics for SDMs in the wind tunnels, due to a mismatch in Reynolds numbers (wind-tunnel Reynolds numbers are at least two orders of magnitude greater than water-tunnel Reynolds numbers). If the flow over the SDM becomes excessively non-linear, then the linearised mathematical model used in Newman's (2011) approach will break down. The data-processing techniques used by Newman may not be able to give meaningful derivatives if the raw data contains excessive perturbations associated with noise and unsteady flow over an oscillating model. Due to the very small flow-induced loads on the water-tunnel model, noise on the raw data has a greater adverse affect on the accuracy of measured derivatives compared with associated wind-tunnel data.

Data measured in the water tunnel were compared with corresponding wind-tunnel data published in the literature to test the goodness of the water-tunnel data. There are significant differences in experimental setups between the different wind-tunnel investigations, including differences in Mach numbers, Reynolds numbers, reduced frequencies of oscillation, oscillation amplitudes, model support systems and tunnel

blockages, resulting in a rather wide scatter in published data. Due to the highly specialised nature of the experiments, there are limited data available for comparison purposes. It is generally agreed that wind tunnels are the preferred option to measure derivatives. However, notwithstanding the above areas of concern for the water-tunnel investigation, measured water-tunnel data were located within the general scatter band of published wind-tunnel data and followed similar trends, suggesting that it is feasible to use a water tunnel to measure derivatives, at least for the SDM, especially if derivatives are required cheaply and quickly. It is believed that this is the first time that longitudinal separated derivatives have been measured using a SDM.

An important finding of the investigation was that it was necessary to carry out tests using a roof suspended above the test section, so that it just touched the water surface, without causing any blockage to the oncoming flow. Without the roof, there were noticeable perturbations in the level of the water surface, resulting in variations in the loads on the model in the form of uncorrelated noise, which affected the quality of the measurements.

Possible future work could be to measure lateral/directional coefficients and derivatives for the SDM, obtained by oscillating the model in roll or pitch, or subjecting it to continuous roll. The current experimental setup could be used without modification for such measurements, but it would be necessary to use a five component strain-gauge balance instead of the two-component balance. Additional possible future work could be to measure surface pressures and acquire images of the flow over the SDM, when it is stationary and in motion, in an attempt to obtain some understanding of the physics of the flow over the SDM. Measurement of parameters and study of the flow could also be extended to other types of aircraft.

9. Acknowledgements

The author is indebted to Daniel Newman from Quantitative Aeronautics, who willingly provided much valuable insight and advice during the acquisition and analysis of the experimental data. Jan Drobik and Simon Henbest gave many helpful suggestions and ongoing support throughout the investigation. Justin Young from QinetiQ developed the software for the operation of the dynamic rig and Daniel Ryan from QinetiQ provided help with the bridge-conditioner unit. Malcolm Jones, Kevin Desmond and Paul Jacquemin helped with the tests. Christopher Jones from QinetiQ drew many of the figures given in the paper. Staff at QinetiQ manufactured rigs and equipment necessary for the tests.

10. References

Alemdaroglu, N., Iyigun, I., Altun, M., Quagliotti, F. & Guglieri, G. 2001 Measurements of dynamic stability derivatives using direct forced oscillation technique. In *Instrumentation in Aerospace Simulation Facilities, 2001, 19th International Congress on Instrumentation in Aerospace Simulation Facilities*, Cleveland, OH, USA, Aug., pp. 275-282.

Alemdaroglu, N., Iyigun, I., Altun, M., Uysal, H., Quagliotti, F. & Guglieri, G. 2002 Determination of dynamic stability derivatives using forced oscillation technique. Paper 2002-0528, *40th AIAA Aerospace Sciences Meeting & Exhibit*, Reno, NV, USA, Jan. 14-17.

Altun, M., & Iyigun, I., 2004 Dynamic stability derivatives on maneuvering combat aircraft model, *J. of Aeronautics and Space Technologies*, Vol. 1, No. 3, Jan., pp. 19-27.

Beyers, M. E. 1985 SDM pitch- and yaw-axis stability derivatives. Paper 1985-1827, *AIAA Atmospheric Flight Mechanics Conference*, Snowmass, CO, USA, Aug. 19-21.

Beyers, M. E., Kapoor, K. B. & Moulton, B. E. 1984 Pitch- and yaw-oscillation experiments on the Standard Dynamics Model at Mach 0.6. National Research Council Canada, National Aeronautical Establishment, *Report LTR-UA-76*, Jun.

Beyers, M. E. & Moulton, B. E. 1983 Stability derivatives due to oscillations in roll for the Standard Dynamics Model at Mach 0.6. National Research Council Canada, National Aeronautical Establishment, *Report LTR-UA-64*, Jan.

Coulter, S. M. & Marquart, E. J. 1982 Cross and cross-coupling derivative measurements on the Standard Dynamics Model at AEDC. Paper 82-0596, *12th AIAA Aerodynamic Testing Conference*, Williamsburg, VA, USA, Mar. 22-24.

Cyran, F. B. 1981 Sting interference effects on the static, dynamic, and base pressure measurements of the standard dynamics model aircraft at Mach numbers 0.3 through 1.3. Arnold Engineering Development Center, *Report AEDC-TR-81-3*, Aug.

Erm, L. P. 2006a Development of a two-component strain-gauge-balance load-measurement system for the DSTO water tunnel. *DSTO-TR-1835*, Platforms Sciences Laboratory, Defence Science and Technology Organisation, Melbourne, Australia.

Erm, L. P. 2006b Development of a dynamic testing capability for the DSTO water tunnel. *DSTO-TR-1836*, Platforms Sciences Laboratory, Defence Science and Technology Organisation, Melbourne, Australia.

Guglieri, G. & Quagliotti, F. B. 1991 Determination of dynamic stability parameters in a low speed wind tunnel. Paper 91-3245-CP, *9th AIAA Applied Aerodynamics Conference*, Baltimore, MD, USA, Sep. 23-25.

Guglieri, G. & Quagliotti, F. B. 1993 Dynamic stability derivatives evaluation in a low-speed wind tunnel. *J. Aircraft*, Vol. 30, No. 3, pp. 421-423.

Huang, X. Z., & Beyers, M. E. 1990 Subsonic aerodynamic coefficients of the SDM at angles of attack up to 90°. National Research Council Canada, National Aeronautical Establishment, *Report LTR-UA-93*, Jan.

Jansson, T. & Torngren, L. 1985 New dynamic testing techniques and related results at FFA. *AGARD FDP Symposium, Unsteady Aerodynamics*, Goettingen, May.

Kabin, S. V., Kolinko, K. A., Khrabrov, A. N., & Nushtaev, P. D. 1995 Dynamic test rig and test technique for the aircraft models unsteady aerodynamic characteristics measurements in high subsonic and transonic wind tunnels, *International Congress on Instrumentation in Aerospace Simulation Facilities, ICIASF '95 Record*.

Newman, D. M. 2011 A technique for measurement of static and dynamic longitudinal aerodynamic derivatives using the DSTO water tunnel, *DSTO-TR-2599*, Defence Science and Technology Organisation, Melbourne, Australia.

Schmidt, E. 1985 Standard dynamics model experiments with the DFVLR/AVA transonic derivative balance. In *AGARD-CP-386 Unsteady Aerodynamic –Fundamentals and Applications to Aircraft Dynamics*.

Suárez, C. J. & Malcolm, G. N. 1995 Dynamic water tunnel tests for flow visualization and force/moment measurement on maneuvering aircraft. Paper 95-1843-CP, *13th AIAA Applied Aerodynamics Conference*, San Diego, CA, USA, Jun. 19-22.

Torngren, L. 1985 Dynamic pitch and yaw derivatives of the SDM. *FFA TN 1985-05*, Bromma, Sweden, Oct.

Ueno, M. & Miwa, H. 2001 New dynamic stability equipment for transonic wind tunnel testing at NAL. Paper 2001-0406, *AIAA 39th Aerospace Sciences Meeting and Exhibit*, Reno, NV, USA, Jan. 8-11.

DEFENCE SCIENCE AND TECHNOLOGY ORGANISATION
DOCUMENT CONTROL DATA

1. PRIVACY MARKING/CAVEAT (OF DOCUMENT)

2. TITLE

An Experimental Investigation Into the Feasibility of Measuring Static and Dynamic Aerodynamic Derivatives in the DSTO Water Tunnel.

3. SECURITY CLASSIFICATION (FOR UNCLASSIFIED REPORTS THAT ARE LIMITED RELEASE USE (L) NEXT TO DOCUMENT CLASSIFICATION)

Document	(U)
Title	(U)
Abstract	(U)

4. AUTHOR(S)

Lincoln P. Erm

5. CORPORATE AUTHOR

DSTO Defence Science and Technology Organisation
506 Lorimer St
Fishermans Bend Victoria 3207 Australia

6a. DSTO NUMBER	6b. AR NUMBER	6c. TYPE OF REPORT	7. DOCUMENT DATE
DSTO-TR-2600	AR-015-088	Technical Report	August 2013

8. FILE NUMBER	9. TASK NUMBER	10. TASK SPONSOR	11. NO. OF PAGES	12. NO. OF REFERENCES
2008/1095269/1	Task Number	Task Sponsor	38	20

13. URL on the World Wide Web

http://dspace.dsto.defence.gov.au/dspace/

14. RELEASE AUTHORITY

Chief, Aerospace Division

15. SECONDARY RELEASE STATEMENT OF THIS DOCUMENT

Approved for public release

OVERSEAS ENQUIRIES OUTSIDE STATED LIMITATIONS SHOULD BE REFERRED THROUGH DOCUMENT EXCHANGE, PO BOX 1500, EDINBURGH, SA 5111

16. DELIBERATE ANNOUNCEMENT

No Limitations

17. CITATION IN OTHER DOCUMENTS Yes

18. DSTO RESEARCH LIBRARY THESAURUS http://web-vic.dsto.defence.gov.au/workareas/library/resources/dsto_thesaurus.shtml

Water tunnel tests, Strain gauges, Dynamic tests, Aircraft Models

19. ABSTRACT

This report gives details of an experimental research investigation carried out in the DSTO water tunnel to see whether it is feasible to measure meaningful aircraft static and dynamic aerodynamic derivatives. These derivatives represent the aerodynamic damping and coupling forces and moments on an aircraft and are used in its equations of motion. A Standard Dynamics Model (SDM), a simplified fighter aircraft configuration, was used for the tests. The SDM was subjected to forced small (±0.5°) sinusoidal pitching oscillations and derivatives were computed from measured model loads, angles of attack, reduced frequency of oscillation and aircraft geometrical parameters. The derivatives obtained in the water tunnel were compared with corresponding published data obtained using SDMs in wind tunnels. Although wind tunnels are the preferred option to obtain derivatives, it was found that it is feasible to use a water tunnel to obtain approximate derivatives, at least for models having SDM-type geometries, especially if derivatives are required quickly and cheaply.